

AD-761 094

RESEARCH AND DEVELOPMENT WORK FOR  
THE GROWTH OF SINGLE CRYSTAL YTTRIUM  
ORTHOVANADATE

Herman G. McKnight, et al

Union Carbide Corporation

Prepared for:

Army Electronics Command

April 1973

DISTRIBUTED BY:



National Technical Information Service  
U. S. DEPARTMENT OF COMMERCE  
5225 Port Royal Road, Springfield Va. 22151

AD 761094

AD



## Research and Development Technical Report

ECOM 0022F

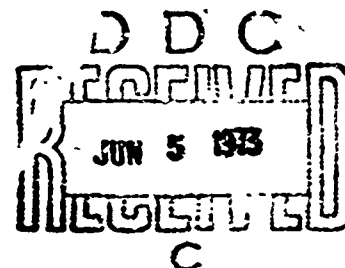
RESEARCH AND DEVELOPMENT WORK  
FOR THE GROWTH OF SINGLE CRYSTAL  
YTTRIUM ORTHOVANADATE

### FINAL TECHNICAL REPORT

By

H. G. McKnight  
L. R. Rothrock

APRIL 1973



Reproduced by  
NATIONAL TECHNICAL  
INFORMATION SERVICE  
U.S. Department of Commerce  
Springfield, VA 22151

Approved for public release. Distribution unlimited.

.....  
**ECOM**

UNITED STATES ARMY ELECTRONICS COMMAND - FORT MONMOUTH, N.J.

CONTRACT DAAB0772-C-12  
UNION CARBIDE CORPORATION  
CRYSTAL PRODUCTS DIVISION  
SAN DIEGO, CALIFORNIA 92123

R-3

ACCESSION &	
RTTB	<input checked="" type="checkbox"/> Main Section
ORG	<input type="checkbox"/> Sub Section
MANUFACTURER	<input type="checkbox"/>
JUSTIFICATION	<input type="checkbox"/>
BY DISTRIBUTION/AVAILABILITY CODES	
BUZL	AVAIL 283/07-314
A	

### NOTICES

### DISCLAIMERS

The findings in this report are not to be construed as an official Department of the Army position, unless so designated by other authorized documents.

The citation of trade names and names of manufacturers in this report is not to be construed as official Government endorsement or approval of commercial products or services referenced herein.

### DISPOSITION

Destroy this report when it is no longer needed. Do not return it to the originator.

## UNCLASSIFIED

Security Classification

## DOCUMENT CONTROL DATA - R &amp; D

(Security classification of title, body of abstract and indexing annotation must be entered when the overall report is classified)

1. ORIGINATING ACTIVITY (Corporate author)  
 Crystal Products Department  
 Union Carbide Corporation  
 8888 Balboa Avenue  
 San Diego, California 92123

2a. REPORT SECURITY CLASSIFICATION  
 UNCLASSIFIED

2b. GROUP

## 3. REPORT TITLE

Research &amp; Development Work for the Growth of Single Crystal Yttrium Orthovanadate

## 4. DESCRIPTIVE NOTES (Type of report and inclusive dates)

Final Technical Report, 1 Oct. 71 - 1 Dec. 72

## 5. AUTHOR(S) (First name, middle initial, last name)

Herman G. McKnight, Larry K Rothrock

6. REPORT DATE April 1973	7a. TOTAL NO. OF PAGES 53	7b. X.O. OF REPS 15
8a. CONTRACT OR GRANT NO. DAAB07-72-C-0022	8a. ORIGINATOR'S REPORT NUMBER(S)	
9a. PROJECT NO. 9 10	9b. OTHER REPORT NUMBER(S) / Any other numbers that may be assigned to this report C -0022-F	

## 10. DISTRIBUTION STATEMENT

Approved for public release: distribution unlimited

11. SUPPLEMENTARY NOTES	12. SPONSORING MILITARY ACTIVITY U.S. Army Electronics Command Fort Monmouth, New Jersey 07703 AMSEL-CT-L-D
-------------------------	--

## 13. ABSTRACT

This program was designed to develop a crystal growth method for yttrium orthovanadate single crystals. The crystal has wide application as a polarizer material. The birefringence is  $\pm 0.226$  which is 1.3 times that of calcite and the birefringence is temperature independent. The crystal is transparent out to 5 microns. The laser damage threshold is  $3\text{GW cm}^{-2}$  significantly higher than calcite.

Glan-Foucault and Rochon polarizers having 1 cm aperture were produced.

Beginning work was centered around using sealed crucible Bridgeman growth. This was deemed necessary in order to maintain a reasonable pressure over the melt and prevent reduction of the vanadium oxide crucible fabrications problems, as well as growth zone control difficulties, suggested that another approach should be considered.

Later work was directed toward Czochralski growth using inert flowing atmosphere, and using strong thermal gradients in the melt to control growth zone. This approach is the one which has been successful. Good quality single crystal boules have been grown along the c-axis and along the a-axis. Regions of the crystal which may be dark after growth can be returned to the original color by oxygen annealing. Boules produced are about 4 cm long by 1.5 cm in diameter. Some boules are water white in color while others have a yellow cast. The reason for this is unknown, but the color does not affect the transmission at the region of interest, namely 1.06. The crystal can be caused to cleave along the (001) face by the usual methods.

DD FORM 1473 1 NOV 68 1280 68 1000 1000  
 REPLACES DD FORM 1473 1 JAN 68 1000 1000  
 OBSOLETE FOR ARMY USE

UNCLASSIFIED

10  
Security Classification

## UNCLASSIFIED

## Security Classification

14. KEY WORDS	LINK A		LINK B		LINK C	
	ROLE	WT	ROLE	WT	ROLE	WT
yttrium vanadate YVO <sub>4</sub> polarizers waveplates birefringence double refraction						

j6

UNCLASSIFIED

TR ECOM 0022F  
APRIL 1973

REPORTS CONTROL SYMBOL  
OSD-1365

RESEARCH AND DEVELOPMENT WORK  
FOR THE GROWTH OF SINGLE CRYSTAL  
YTTRIUM ORTHOVANADATE

FINAL TECHNICAL REPORT

DECEMBER 1972

CONTRACT NO. DAAB07-72-C-0022

PROJECT NO. C8-1-04324-03-C8-CA

PREPARED BY

H. G. McKnight  
L. R. Rothrock

Approval for public release; distribution unlimited.

UNION CARBIDE CORPORATION  
MATERIALS SYSTEMS DIVISION  
CRYSTAL PRODUCTS DEPARTMENT  
8888 BALBOA AVENUE  
SAN DIEGO, CALIFORNIA 92123

For

U.S. ARMY ELECTRONICS COMMAND  
FORT MONMOUTH, NEW JERSEY

ic

## FOREWORD

This Final Technical Report presents the work done under Contract No. DAAB0772-C-0022. The reported work covers the time from 1 October 1971 to 1 December 1972. The title of the work is "Research and Development Work for the Growth of Single Crystal Yttrium Orthovanadate". The work was performed for the Electronics Components Laboratory, U.S. Army Electronics Command, Ft. Monmouth, New Jersey. The program was monitored by Mr. John Strozyk as Contracting Officer.

Crystal Products Department of Union Carbide Corporation conducted the program at San Diego, California.

The initial months of the program were conducted by G. A. Keig and D. E. Witmer. The final months were performed by H. G. McKnight and L. R. Rothrock. H. L. Landt and K. T. Beck assisted with the boule growth and polarizers were fabricated by R. Szymanski and A. R. coated by R. E. Wilder.

Birefringence, optical work and polarizer design were done by L. G. DeShazer, University of Southern California, Los Angeles, California.

id

## TABLE OF CONTENTS

	<u>Page</u>
I. INTRODUCTION	1
II. YTTRIUM VANADATE GROWTH	3
A. Summary of Previous Growth Efforts	4
B. Crystal Growth Method Investigation	4
C. Sealed Crucible Design and Fabrication	6
D. Testing of the Crucible Assembly	9
E. Sealed Crucible Furnace Construction	9
F. Sealed Crucible Crystal Growth	12
G. Spontaneously Seeded Open Crucible Growth	15
III. CZOCHRALSKI GROWTH	19
IV. APPLIED DESIGN OF $\text{YVO}_4$ POLARIZING DEVICES	22
A. Introduction	22
B. Material Quality	23
C. Surface Reflection and Scattering Losses	23
D. Reflection Losses Between Prisms	24
E. Dimensional Stability and Prism Alignment	25
F. Polarizing Devices of the Double-Refraction Type	26
G. Practical Considerations for Polarizer Designs	43
V. PROPERTIES OF YTTRIUM ORTHOVANADATE	46
A. Optical Properties	46
B. Physical Properties	48

## LIST OF FIGURES

	<u>Page</u>
Figure 2-1. Phase Diagram - System $Y_2O_3$ - $V_2O_5$	5
Figure 2-2. The Vanadium-Oxygen System	7
Figure 2-3. The First Iridium Crucible	8
Figure 2-4. The Contract Configuration Crucible	10
Figure 2-5. Modified Graphite Astro Furnace Pedestal	11
Figure 2-6. Third Run Core Drilling	14
Figure 2-7. Second Phase Inclusions in $YVO_4$	17
Figure 2-8. Section Through Core Drilling	18
Figure 3-1. Czochralski Crystal Growth	21
Figure 4-1. Glan-Foucault Polarizer	27
Figure 4-2. Critical Angle as a Function of Wavelength	29
Figure 4-3. Reflectivity as a Function of Incident Angle for $YVO_4$	30
Figure 4-4. Reflectivity as a Function of Incident Angle for Calcite	30
Figure 4-5. Glan-Foucault Polarizer Design Schematic	32
Figure 4-6. Rochon Prism	33
Figure 4-7. $\langle 001 \rangle$ $YVO_4$ Boule for Glan-Foucault Prisms	36
Figure 4-8. Schlieren Image Through Glan-Foucault Polarizer	37
Figure 4-9. Crossed Polar Photographs Through Glan-Foucault Polarizer	38
Figure 4-10. $\langle 100 \rangle$ $YVO_4$ Boule for Rochon Prisms	42
Figure 5-1. Change in Refractive Indices as a Function of Temperature for Single Crystal $YVO_4$	49
Figure 5-2. Absorption Coefficient for $YVO_4$ Plotted Versus Wavelength	50
Figure 5-3. Comparison of Laser Damage Resistance for Calcite and $YVO_4$	52

## LIST OF TABLES

	<u>Page</u>
<b>TABLE I-1.</b> Principal Optical and Physical Properties of Yttrium Orthovanadate	2
<b>TABLE IV-1.</b> The Relative Intensities of Transmitted and Reflected Rays Within the Air Gap for Different Prism Designs.	34
<b>TABLE IV-2.</b> The Angle of Separation for Polarized Rays Emerging from a Rochon Polarizer Cut at Different Prism Angles $\beta$ .	41
<b>TABLE V-2.</b> Refractive Index as a Function of a Wavelength for Single Crystal $\text{YVO}_4$ .	47

ABSTRACT

The growth of yttrium orthovanadate large single crystals is reported. The two most promising crystal growth methods were investigated. The Bridgman method shows some promise with further development in vendor state-of-the-art, iridium fabrication technology, and a refinement in crucible design. The Czochralski method successfully yielded large "a" and "c" axis boules. Growth parameter development is described and the results evaluated.

Glan-Foucault and Rochon polarizers have been assembled from prisms fabricated from these boules and tested.

## I. INTRODUCTION

In the year 1809, E. L. Malus published a paper covering his discovery of the polarization of light by reflection from a glass surface. Christiaan Heuygens had described, in 1678, the double refraction observed in calcite and other crystals in terms of his new wave theory. He also discovered, although he did not explain, the phenomena of polarization. The Malus publication gave impetus to the optical investigation of natural crystals by Sir David Brewster and others. In 1810 Malus published a memoir on the theory of double refraction in crystals.

Development rather quickly produced a number of polarizer designs which have remained essentially unchanged to the present day, with extensive use in optical instrumentation. These designs still bear the names of their inventors - Foucault, Nichol, Ahrens, Taylor, Thompson and others. Many of these designs depended upon the assembly of prisms in a manner which develops a reflecting interface between the parts. Another class of polarizers such as those designed by Rochon and Wollaston needed a non-reflecting interface and depended upon crystal refraction anisotropy for separation of the ordinary from the extraordinary ray. The ideal interface for Rochon and Wollaston designs is an optical contacting between the two prisms which form the polarizer. It is logical to usually find these polarizers made from quartz because of the stringent optical flatness tolerances necessary to achieve an optical contact. The softness of calcite makes it very difficult to achieve this degree of flatness.

A further disadvantage to the present day use of calcite is the rapidly depleting supply of large size, optically clear crystals.

Crystalline yttrium orthovanadate ( $\text{YVO}_4$ ) has not been found in natural occurrences; but a few small crystals have been laboratory grown in recent years. Their properties have been studied, in the doped variations, as laser hosts. Four properties of  $\text{YVO}_4$  single crystals make the material a superior substitute for calcite in polarizer applications.

Yttrium vanadate is a positive, uniaxial crystal with a birefringence of +0.226, approximately 25% higher than the value of -0.172 for calcite. The positive  $\text{YVO}_4$  birefringence had previously been reported by others, with the wrong sign<sup>1</sup>. The refractive index of  $\text{YVO}_4$  is higher than that of calcite across the usable spectrum and shows values of 1.958 and 2.168 at 1.66 microns. The refractive index of  $\text{YVO}_4$  remains relatively constant with temperature to 300°K for both the ordinary and extraordinary rays while the temperature coefficients differ substantially for each ray (Table I-1) in calcite.

	<u>YVO<sub>4</sub></u>	<u>CaCO<sub>3</sub></u>	<u>Quartz</u>
Crystal System	Tetragonal	Rhombohedral	Hexagonal
Index of Refraction (n <sub>η</sub> )			
Ordinary	2.000	1.653	1.544
Extraordinary	2.226	1.487	1.553
Dispersion (n <sub>F</sub> - n <sub>C</sub> )			
Ordinary	0.042	0.013	0.009
Extraordinary	0.059	0.006	0.009
Temperature Coefficient (dn/dt) (at room temperature)			
Ordinary	+3.9 x 10 <sup>-5</sup>	+0.2 x 10 <sup>-5</sup>	-0.5 x 10 <sup>-5</sup>
Extraordinary	+3.9 x 10 <sup>-5</sup>	+1.2 x 10 <sup>-5</sup>	-0.6 x 10 <sup>-5</sup>
Transmission Range (microns)	0.4 - 3.8	0.35 - 2.1	0.4 - 2.2
Hardness, Knoop HN	480	135	710
Melting Point	1810 ± 25°C	1339°C at 102.5 atm.	1713°C

Table I-1. Principal Optical and Physical Properties of Yttrium Orthovanadate:  
Comparison is made with Calcite and Quartz.

The antireflection coating of polarizers requires multiple component layers to match calcite at 1.06 microns transmission, while conventional single layer magnesium fluoride provides a good match to  $\text{YVO}_4$ .

The useful transmission range of yttrium vanadate extends to 5 microns which makes polarizers possible in the important 2 to 5 micron range in laser systems.

The hardness of 450 KHN for  $\text{YVO}_4$  is equivalent to that of frequently used optical glasses and permits the use of the same fabrication techniques. Optical contacting is more practical with  $\text{YVO}_4$  because of this and a lesser tendency to cleave than in calcite. Surface finishing of optical quality is considerably easier with  $\text{YVO}_4$ .

Other property upgrading by yttrium vanadate is of particular interest when applied to laser systems. Laser damage resistance has been good to  $3000 \text{ MW/cm}^2$  while calcite suffers serious damage in the 900 to  $1200 \text{ MW/cm}^2$  range. The damage has been largely surface damage with  $\text{YVO}_4$  but calcite damage has been internal. There is an increase of 30% in beam splitting in a Rochon polarizer with  $\text{YVO}_4$  and a two orders-of-magnitude reduction in the energy reflected in the air gap of a  $\text{YVO}_4$  Glan-Foucault polarizer.

These properties clearly demonstrate the superiority of  $\text{YVO}_4$  over both calcite and quartz for polarizers, but active application of yttrium vanadate to the production of such polarizers has not been possible in the past because of the difficulty of reproducibly growing undoped  $\text{YVO}_4$  of suitable optical clarity and of sufficient size to avoid compromising the systems on which they were to be used.

The research and development work described in this contract shows that large crystals of oriented yttrium vanadate, having the required optical properties can be grown and it has been demonstrated that both Glan-Foucault and Rochon polarizers can be produced with good optical fabrication techniques.

## II. YTTRIUM VANADATE GROWTH

Yttrium orthovanadate has a body-centered tetragonal zircon structure with lattice parameters of  $a = 7.114 \text{ \AA}$  and  $c = 6.258 \text{ \AA}$ .<sup>2</sup> Its structure is isomorphous with the rare earth vanadates in the series from cerium to lutetium<sup>3</sup>.  $\text{YVO}_4$  is not a naturally occurring mineral. It was first synthesized by Goldschmidt and Haraidsen at the University of Oslo in 1928.<sup>4</sup>

$\text{YVO}_4$  has become of interest recently for three primary reasons. First, as a powder doped with europium, it provides a brilliant red cathodoluminescent phosphor with color coordinates  $X = 0.670$ ,  $Y = 0.330$  (pure

spectral red).<sup>5,6</sup> Second,  $\text{YVO}_4$  in the single crystal form is of interest as a possible laser host for rare earths such as europium, dysprosium, neodymium and others.<sup>7</sup> Third, the polarizing ability of yttrium vanadate is outstanding.

The fluorescent properties of different dopings is of interest. Both the pure yttrium vanadate and the europium doped material fluoresce brilliantly under ultraviolet light. The pure material fluoresces a pale buff color while the europium doped material fluoresces a bright red. Interestingly, the addition of neodymium to the pure  $\text{YVO}_4$  suppresses all fluorescence in ultraviolet light.

#### A. SUMMARY OF PREVIOUS GROWTH EFFORTS

Based upon the phase equilibrium diagram for the  $\text{Y}_2\text{O}_3$ - $\text{V}_2\text{O}_5$  system (Fig. 2-1), yttrium vanadate ( $\text{YVO}_4$ ) melts congruently at  $1810^\circ\text{C}$ . Rubin and Van Uitert<sup>8</sup> have grown crystals from the melt using iridium crucibles heated in an oxyhydrogen furnace. The process was also studied by Doss and Bolin<sup>9</sup> at about the same time.

The experiments using oxyhydrogen heating all report the formation of heavy surface crusts over the melt. The recommended procedure for growth under these conditions was designed to permit the surface formation of this crust, which was largely oxygen deficient  $\text{YVO}_4$  of variable composition. A hole was then punched through the crust and the crystal grown through this hole while directing a stream of inert gas, usually argon, onto the melt surface and the seed.

The most recent experimental  $\text{YVO}_4$  growths prior to this contract were done by Witter and Smith in 1970<sup>10</sup>. Small single crystals of undoped  $\text{YVO}_4$  were grown in an RF station with impingement of a stream of argon on the melt surface at the solid/liquid interface. The yield was suitable for optical measurements and fabrication into small polarizers.

The difficulty of controlling the formation of second phase oxygen deficient  $\text{YVO}_4$  during these experiments resulted in the development of a sealed crucible design for the Bridgman growth investigation phase of this contract. A literature search and computer calculations indicated acceptable equilibrium conditions could be achieved at crystal growth temperature and moderate pressures in a vessel sealed under vacuum, provided that the vessel was constructed of iridium.

#### B. CRYSTAL GROWTH METHOD INVESTIGATION

Several potential crystal growth methods were investigated experimentally and through a literature search. The vanadium oxygen system

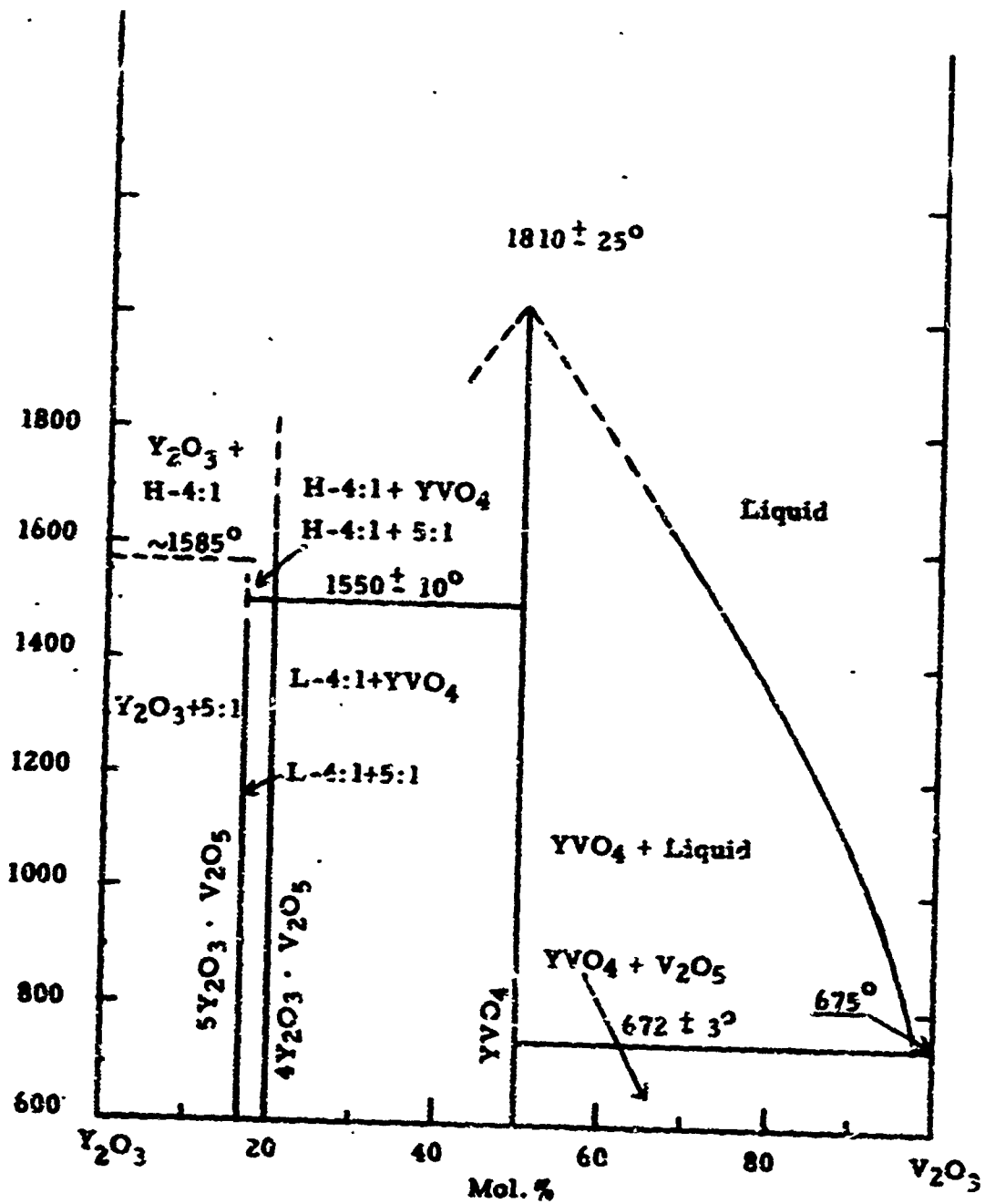


Figure 2-1. Phase Diagram-System  $\text{Y}_2\text{O}_3$ - $\text{V}_2\text{O}_5$   
 E. M. Levin, J. Am. Ceram. Soc., 50 [7] 381 (1967)

11  
was reviewed in depth by J. Stringer <sup>11</sup> in 1964. This work indicated a complex series of vanadium oxides with the loss of oxygen (Figure 2-2). It was evident that oxygen deficiency could be expected to be a major problem in the  $\text{YVO}_4$  compound, as well. The methods of Rubin and Van Uitert <sup>8</sup>, Doss and Bolin <sup>9</sup>, and Witter and Smith <sup>10</sup> were studied as they related to decomposition and the general approach to Czochralski growth. With the exception of a few experiments by Witter in 1970, all of the information on Czochralski growth was derived from parameters characteristic of oxy-hydrogen gas heated furnaces. Witter applied this same technology to RF heated equipment with somewhat similar results. The useful yield was small crystals, darkly colored and less than repeatable performance. A concept of sealing the starting material within an iridium crucible could visualize the generation of the few atmospheres of pressure necessary to create equilibria in the presence of iridium oxide formed from the free oxygen liberated by the decomposition reaction.

The consideration of the Bridgman technique resulted in several experiments utilizing a sealed iridium crucible. Weld failures were the usual reason for experiment termination but small crystallites of yttrium vanadate were grown. Although this concept is still considered sound, it did not produce the success which had been predicted for it. The investigation served to provide an awareness of two ancillary developments which must precede any further work in this method. First, further development of iridium metal fabrication technology is necessary to provide a sound vessel free of voids, pores, and laminations. This is a vendor problem, not solvable within the time limit of this contract. Second, a new design of vessel must be developed which will permit the seeding zone to remain free of precipitating second phase material during the early stages of the growth.

A further method was anticipated to define the phase-temperature relations in the useful growth zone of the phase diagram. This method was one of slowly cooling the charge in an open iridium crucible from a point a few degrees above the melting temperature to complete solidification. The results from a series of these runs developed the preferred seeding temperature and furnished a guide to the appearance of the thermal convection lines and the location of the seeding spot.

### C. SEALED CRUCIBLE DESIGN AND FABRICATION

The first iridium crucible (See Figure 2-3) was fabricated from material available in-house. It was 1" O.D. by 6-1/4" long, including a conical closure at the seeding end and a disc closure at the opposite end. The fabrication, although consisting of several iridium pieces, was expertly TIG welded in our facilities. During this construction, the contract configuration crucible was designed and fabrication ordered from our iridium vendor. The contract crucible is 1" I.D. by 6-3/8" long, including a 1/2" I.D. by 1" long

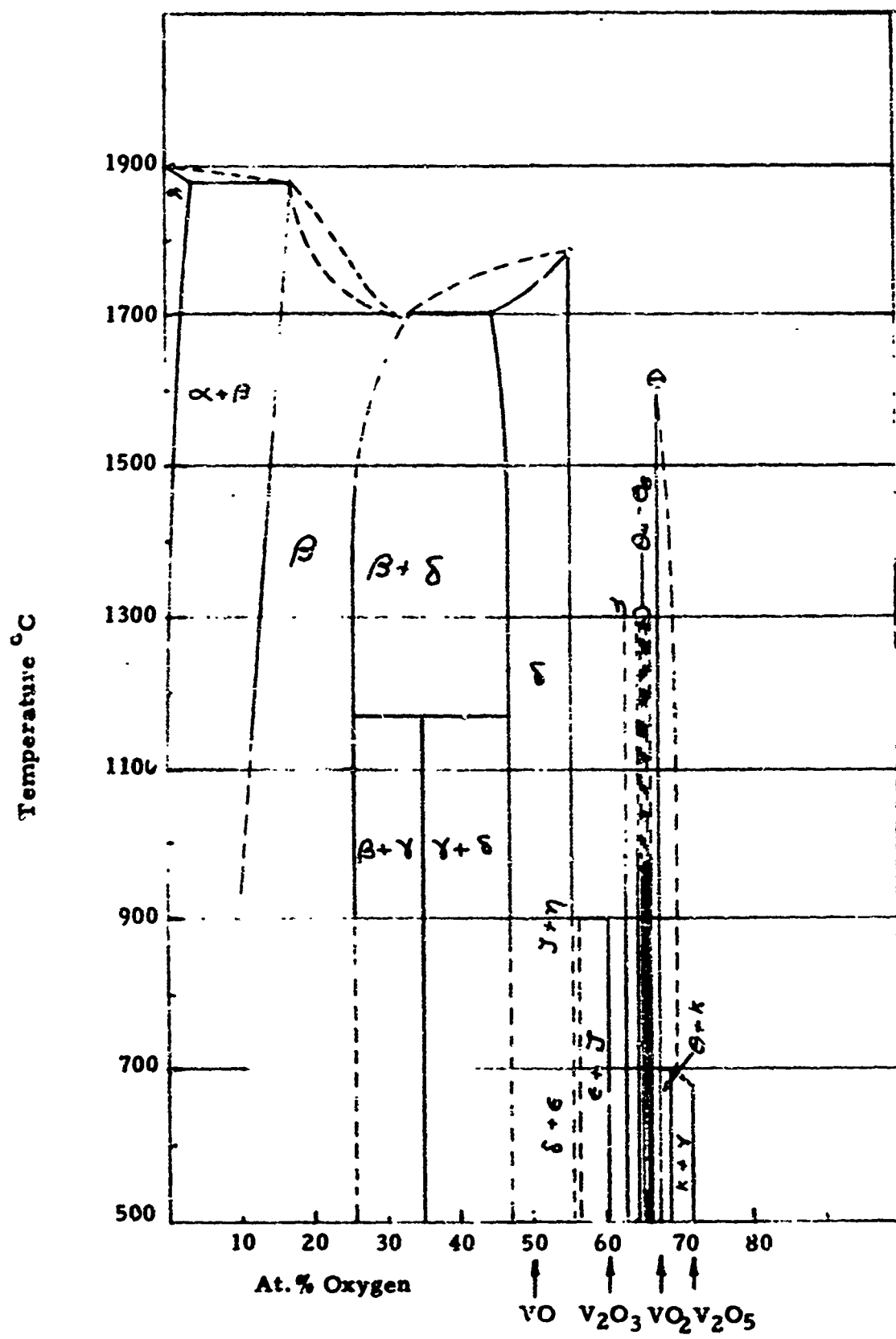
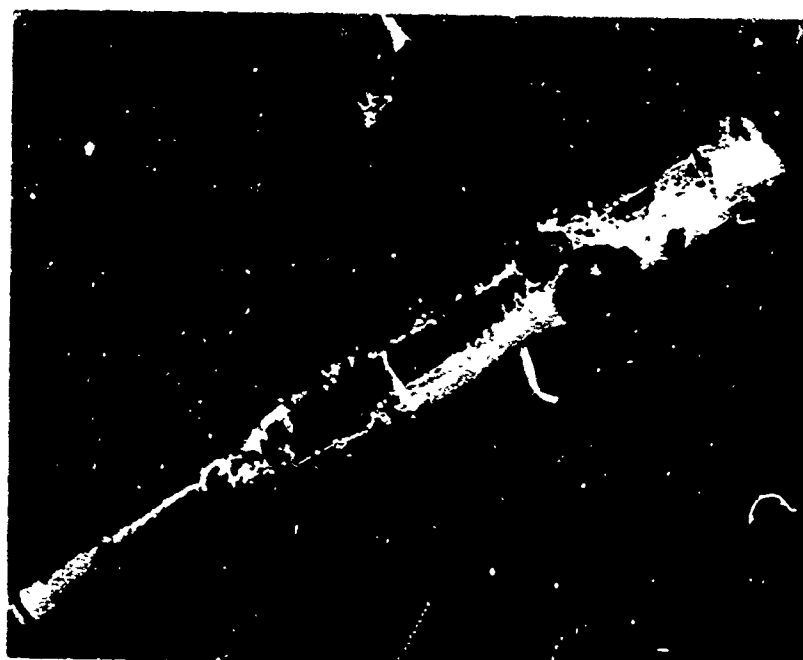


Figure 2-2. The Vanadium-Oxygen System  
R. S. W. Rostoker - The Metallurgy of Vanadium - Wiley



After First  
Test Run



After First  
Full Charge  
Run with Open  
Seeding Tube  
Added

Figure 2-3. The First Iridium Crucible

seed tube at the bottom. This was welded to the upper tube through a transition piece which is a 60° included angle funnel shape. (See Figure 2-4). The contract crucibles were produced of iridium by Engelhard Industries and the final closures were electron-beam butt welds produced by Solar Division of International Harvester Corp. To facilitate the placement of the electron-beam weld in the most efficient position, the upper closure of the crucible was produced as a flat disc which was TIG welded to the side wall in a continuous fusion weld. This joint was then checked on a Veeco model MS-90 helium leak detector. A saw cut 1/8" below the weld then became the closely mated interface surfaces for the final E. B. weld.

#### D. TESTING OF THE CRUCIBLE ASSEMBLY

Testing of the charged crucible, after E. B. welding, was accomplished by pressurizing the outer surfaces of the crucible under ten atmospheres of helium gas. The crucible was then transferred to a flask of water held at 95°C to observe bubbling from any porosity. A final inspection was then made for helium leakage by placing the crucible in a small bell jar on the inspection test port of the leak detector.

#### E. SEALED CRUCIBLE FURNACE CONSTRUCTION

A graphite element furnace, having graphite insulation, supplied by Astro Industries (Model 1000A) was used for the growth efforts in the earlier part of the program. The compatibility of iridium was tested in this furnace over the temperature range to 1850°C. No reaction was detectable.

A graphite pedestal was constructed for the furnace to serve both as a support for the crucible and as a variable heat sink, adjustable by gas flow change (See Figure 2-5).

A later modification included the use of a continuous alumina muffle tube having an alumina pedestal construction for the crucible. This effectively separated the crucible from the effects of the carbonaceous atmosphere within the heating chamber.

A power feedback stabilized power supply for this furnace included R. I. Controls Company's Paramac two-mode controller and Datatrak programmer modified to program both power and the variable flow of gas to the heat sink. The Paramac controlled the Astro Industries' SCR power supply which was transformer coupled to the graphite heating element.

Temperature monitors consisted of two pt-rh thermocouples in the heat sink gas stream arranged to permit calorimetry experiments. In

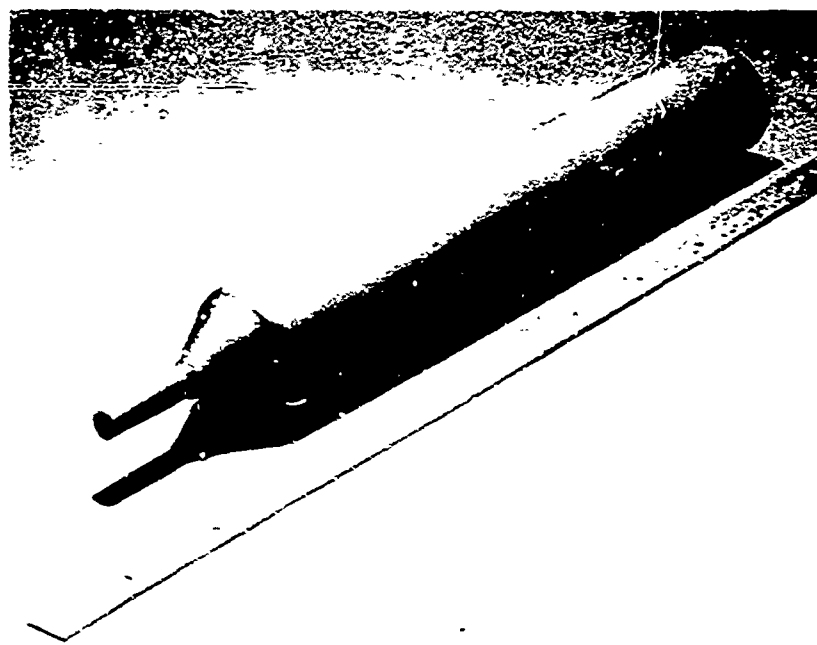


**Figure 2-4. The Contract Configuration Crucible**

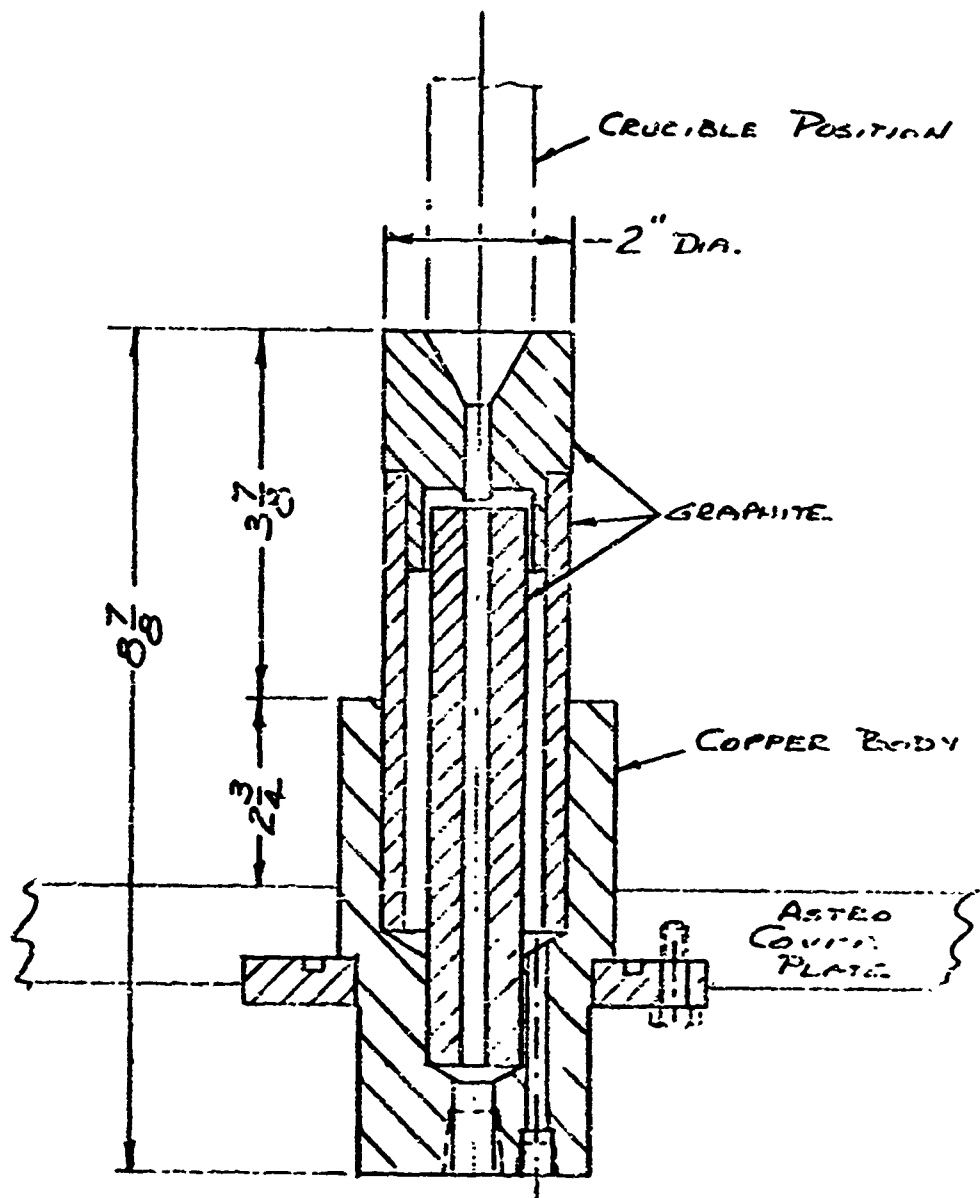


Figure 2-5. Modified Graphite Astro Furnace Pedestal

addition, a two-color Coloratio optical pyrometer was sighted through a purged window to detect the radiation from the top of the crucible. A side port was also used for hand-held Leeds and Northrup pyrometer sightings. Recorder traces of temperatures at three points, gas pressures at two points, and a current curve were recorded on a six-point Rikadenki chart recorder with 30 MV span.

#### F. SEALED CRUCIBLE CRYSTAL GROWTH

The initial growth was made in the original test crucible to which a seeding tube had been added (Figure 2-3). The crucible was sealed except for a loose fitting plug of iridium at the seeding tip. A seed and a small amount of  $\text{YVO}_4$  charge was used to determine the temperature profile effect in the seed zone. Evidence of decomposition due to open construction was apparent in furnace atmosphere and in the charge residue, which was black polycrystalline.

The second run was made in the sealed contract crucible configuration with a full charge of compacted, prereacted  $\text{YVO}_4$ . This run was made on the previously determined program and resulted in the desired degree of melt-back. Growth was finely polycrystalline with two phases present and dispersed into a macroscopically uniform gray color matrix with a thin black crust at the top of the melt. The two phases were composed of tiny clear crystallites showing rectangular cleavage prisms along with the second phase which was black and more dendritic in habit.

The crucible charge was diamond core drilled and acid cleaned between each run, recharged and rewelded for the next run.

During the second run, some leakage occurred at previously repaired spots and it was apparent that alloying with the iridium had occurred. The damage was extensive over a length of 1-1/4" of the crucible wall. This zone was cut away and emission spectrographic analysis of sections cut from the alloyed area showed major vanadium content with traces of other elements. Background was provided by a powder sample of the charge and a test piece from an unalloyed portion of the crucible.

The conclusions drawn from the data showed that the leakage points were minor pores in the iridium metal which served as stress raisers in the path of structural defects such as lamination folds and laps produced in the original fabrication breakdown of the ingot.

Leakage through the pores expelled liquid under pressure which rapidly reacted with the naturally carbonaceous atmosphere of the graphite lined furnace. The vanadium oxide component of the charge was reduced to

vanadium metal which attacked the crucible wall at the point of exit forming a low melting point eutectic alloy which further weakened the wall with the formation of local cracks.

The role of principal investigator was assumed at this time by H. C. McKnight with the resignation of D. W. Witter to accept an opportunity elsewhere.

A reappraisal of the program was made at this time resulting in a decision to correct the deficiencies which became apparent during the first experiments.

The crucible was repaired by dissection of all alloyed areas and replacing with virgin iridium material by TIG welding. After charging with presintered  $YVO_4$  the crucible was leak checked and installed in the chamber for the third run.

The third run was completed in a fully programmed manner. At the completion of the run it was noted that a large crack had opened in the vicinity of a repair weld joint and outer surface contamination was extensive, making it inadvisable to attempt any further runs. A new crucible was ordered and preparations were made for the investigation of the problems during the lead-time wait for the new crucible.

Core drilling of the third run charge disclosed the stratification shown in Figure 2-6 and noted below.

1. Part of the original "c" axis seed remained unmelted.

2. Oriented crystallization proceeded from the point of seed melt-back for approximately 1" to a point just above the transition of the cone to the side wall of the crucible. This zone was cracked extensively into small cleavage rectangular prisms interspersed with black second phase amorphous and dendritic inclusions which were the probable cause for the extensive cleavage observed. Above this zone, beginning on a sharp demarcation plane was a very fine grain, gray, polycrystalline layer about 1" deep. Above this the balance of the charge was composed of large, random orientation, black crystals.

Subsequent analysis has identified the various zones and the reason they existed has been inferred from later experiments. The black phase was oxygen deficient yttrium vanadate of varying composition. The clear crystals were yttrium vanadate with black second phase rejected to the grain boundaries which tended to coincide with cleavage planes.

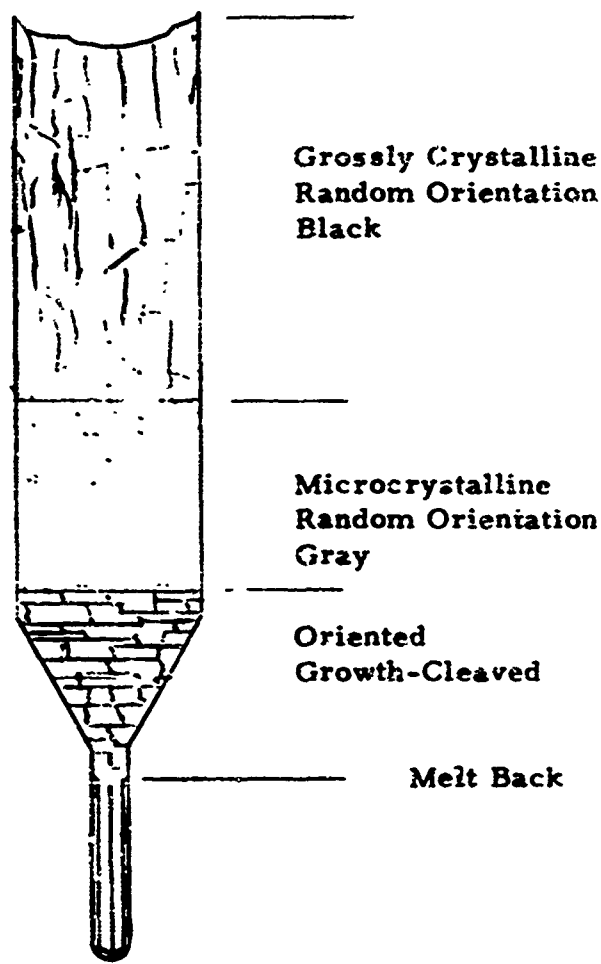


Figure 3-6. Third Run Core Drilling

The gray, finely polycrystalline zone consisted of microcrystals of  $\text{YVO}_4$  in excessive amounts of decomposition product which stopped the oriented growth. Although no density measurements were attempted, gravity distribution of the second phase dendrites indicated in later experiments that the density was higher than the melt and further, that the melting point of the oxygen deficient phase could be placed at least  $130^\circ\text{C}$  higher than the crystallizing  $\text{YVO}_4$ .

These conclusions were reached during the waiting period while the new crucible was being fabricated and were based upon a series of eight experiments in sealed iridium capsules  $3/8''$  O.D. by  $1-1/4''$  long. These tests cast serious doubt on the ability of state-of-the-art iridium fabrication to assure the production of pore-free, lap-free material from which to fabricate crucibles, and the  $\text{YVO}_4$  contract was too far advanced to engage in a basic crucible materials development within the available time remaining for the program. As a result, further work on Bridgman growth was terminated.

#### G. SPONTANEOUSLY SEEDED OPEN CRUCIBLE GROWTH

The method which appeared most useful for experimentally determining parameters, and was eventually a deciding factor in the future development of this program, can best be described as a spontaneously seeded growth having the following major characteristics. The growth was instituted within an open top iridium crucible heated by an RF generator. The charge consisted of  $\text{YVO}_4$  powder type 1533-1, undoped, as supplied by General Electric Company. Most of the melts were made with a stoichiometric starting material, but experiments were also conducted which varied the composition from vanadium rich to yttrium rich starting materials. No advantage was noted from these deliberate changes to the compound.

The powder charge was brought to temperature to establish a melt and then a gradual reduction of input power resulted in the formation of a small floating crystal island in the coolest part of the melt, which was the geometric center of the melt surface. After equilibration of the system, power was programmed down at a very slow rate resulting in a freeze over of the top of the melt and propagation of the island crystal orientation through the upper part of the melt.

Core drilling permitted the cleaving of individual rectangular prisms of various sizes from the mass for further study. Fifteen crystallization experiments were conducted in this manner.

Spontaneous growth preferred either  $\langle 001 \rangle$  or  $\langle 100 \rangle$  growth direction with well developed cleavage planes parallel to both axes. Second

phase segregation occurred along small grain boundaries which coincided with cleavage surfaces.

The second phase was black in color, and when well developed, was dendritic in habit (Figure 2-7). This phase was determined to be stoichiometric in its metal content and oxygen deficient. Experiments on heavy inclusions within a  $\text{YVO}_4$  matrix did not yield an exact melting point, but it was estimated to be near  $1950^\circ\text{C}$  and would be expected to vary with oxygen content.

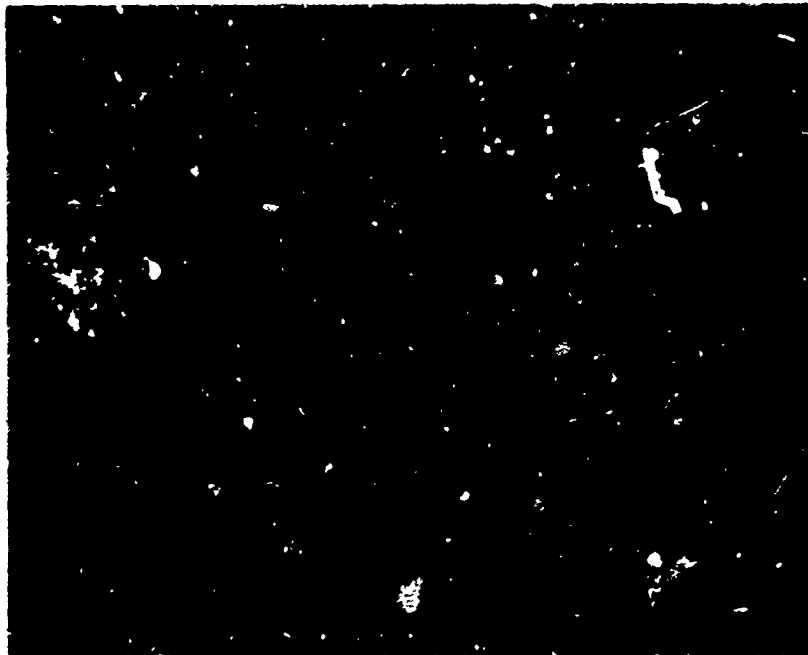
The second phase was also inferred to have very low solubility in the melt because of the distribution of dendrites within the crystallized structure. These inclusions were of smaller mass in the upper crystallization which had formed first, and more dense and dendritic as the distance below the surface increased. A heavy deposit of dendrites in matrix (Figure 2-8) was always found in the bottom of the crucible and located in zones free from strong convection currents.

The  $\text{YVO}_4$  crystals were deep yellow to dark brown depending upon their melt history and position below the surface. The lighter colors were in the first crystallization and the darker ones in the lower levels. The oxygen deficiency in the crystals could be somewhat compensated by heat treatment for several hours at  $1450^\circ\text{C}$  in oxygen with the background coloration of the crystals tending toward light yellow with time and the inclusions being reduced in apparent size and density. The sites occupied by dendrites could be identified after heat treatment by their ghost outlines observed during phase contrast microscopy. Heat treatment in a bed of powdered  $\text{Y}_2\text{O}_3$  showed slight improvement over the  $\text{O}_2$  treatment at the same temperature and time cycle. It is interesting to note that a crust of yellow color was developed in the yttria powder at the contact with the  $\text{YVO}_4$ . No attempt was made to identify the compound.

It appeared, on the basis of these experiments, that the Bridgman concept had the capability of producing crystallization in the  $\text{YVO}_4$  system but not in the configuration proposed, for the following reasons.

1. The black, oxygen deficient, phase was formed even under the best sealing we had done, during the period before decomposition equilibrium was attained.

2. The oxygen deficient phase, having a higher melting point and a limited solubility in the  $\text{YVO}_4$  melt, could be expected to settle in the seed area and interfere with high quality crystal growth.



40X  
Dark Field



250X  
Transmission  
Lighting

Figure 2-7. Second Phase Inclusions in  $\text{YVO}_4$



**Figure 2-8. Section Through Core Drilling  
Self-Seeded Crucible Growth**

3. The integrity of the iridium metal is in question at the current state of art of initial compaction, ingot breakdown, and rolling and fabrication technology, with the main problems being porosity and metal weakness at folds and discontinuities in the solid structure. Further, the threat of vanadium contamination in the event of a rupture made good repair welds seem unlikely.

### III. CZOCHRALSKI GROWTH

The other method of growth which seemed to hold promise was the Czochralski process. A few short, small diameter crystals had been grown at Crystal Products in the previous year, with troubles which appeared to be due to decomposition. Prior Czochralski work at Union Carbide Speedway Laboratory had been successful in producing small crystals in gas flame stations with yield being the major uncertainty. However, this work by Dessa and Bolin did seem to offer a solution to the production of Glan-Foucault and Rochon prisms of  $\text{YVO}_4$ .

Development work in the Czochralski method on this contract was done, for most of the runs, on a 25KVA RF generator. The station was built up of zirconia tubes to contain zirconia grog and arranged to form efficient radiation shielding around the 1-3/4" diameter by 2-1/4" deep iridium crucible. The furnace was enclosed in a bell jar for atmosphere control.

All previously published data had indicated a strong stream of argon gas was to be directed at the surface of the melt at the seeding point and that oxygen added to the inert bell jar atmosphere was desirable to keep the seed transparent. Our starting parameters included a nitrogen stream rather than argon and a bell jar atmosphere of nitrogen plus 20,000 ppm  $\text{O}_2$ .

Four runs were required to familiarize our technicians with the unusual seeding technique needed to institute crystal growth. The fourth run resulted in a start but the growth was polycrystalline. The next two runs were not successful growth runs but were useful in adjusting the crucible position in the work coils and manipulating the gas discharge tube to a proper impingement. The seventh run was single crystal after a poor start and was "cork-screw" shaped. Some improvement in size and quality was observed in the crystals from the next six runs. On the fourteenth run the program was changed to provide for a gradual increase in diameter with time. This boule did not show the strong tendency for the growth axis to wander, and it was repeated in the next experiment with the same result.

A series of experiments was begun on the seed cooling gas stream. The direction of the stream was changed to impinge normal to the seed rotation axis, slightly above the melt surface, bringing noticeable improvement in the growth habit without resorting to diameter change to gain stability.

Run #19 crystal was intentionally frozen in the crucible charge. It was uniformly honey colored with the single crystal propagating into the melt as wide as the crystal and as long as the diameter of the crucible and extending nearly to the bottom of the crucible. It was also discovered that the gas discharge port had been fouled during powder loading and therefore was not effective during growth.

Run #20 was the first without strong gas impingement on the boule and confirmed the parameters predicted by Run #19. The boule was good quality with step facets on one side parallel to the  $\langle 001 \rangle$  axis; pale yellow.

Run #21 was  $\langle 001 \rangle$  and was grown from the same melt as Run #20. The program produced a larger boule of more uniform cross section which was a rounded corner square. Some misorientations were produced during seeding; tan coloration.

Run #22 was the first  $\langle 100 \rangle$  growth. It was pale yellow and had one crack parallel to the growth axis; optical quality was good.

Run #23 produced a somewhat darker boule which offset sharply after about  $1\frac{1}{2}$ " of growth. It was terminated because of mechanical interference between the offset and the crucible lid.

Run #24 was  $\langle 100 \rangle$  and was the longest boule grown on this program. The color was golden yellow and optically clear over the first three inches. The final inch of growth contained second phase inclusions. The boule offset about each  $3/4$ " length to produce a crankshaft effect. This boule was used for the Rochon prism and also for two good quality seeds.

Run #25 was terminated. Growing boule was hitting crucible lid.

Run #26 was  $\langle 001 \rangle$  of substantial size, about  $3/4$ " square with rounded corners. The growth length was  $2-7/16$ " of which the last  $1/4$ " contained second phase inclusions. The balance of the material was of good optical quality, golden yellow. It was used to produce Glan-Foucault prisms.

Run #27 was  $\langle 100 \rangle$ . During the shouldering, two twins were formed which grew alongside the major crystal which was of good optical quality.

Figure 3-1.  
Czochralski Crystal Growth

<u>SD 218-</u> <u>Experimental</u> <u>Growth Serial</u>	<u>Boule Axis</u>	<u>Cross Section</u> <u>Size - Inches</u>	<u>Length</u> <u>Inches.</u>	<u>Growth</u> <u>Interface</u>	<u>Comments</u>
-20	$\langle 001 \rangle + 15^\circ$	5/16 x 7/16	.. 1/4	1/8" Conical	First run without strong gas cooling. Pale yellow. Good quality.
-21	$\langle 001 \rangle$	3/4 x 3/4	3	1/8" Conical	Misorientations at two corners.
-22	$\langle 100 \rangle + 10^\circ$	5/8 x 5/8	1.5/8	Slight Cone	Pale yellow with one longitudinal crack.
-23	$\langle 001 \rangle$	5/8 x 5/8	1	1/16" Conical	Strong dog leg after 1/2" growth.
-24	$\langle 100 \rangle$	1/2 x 5/8	4	1/16" Conical	Golden yellow. Dog leg reversing after each 3/4" length. Used for Rochon prisms.
-25	$\langle 100 \rangle$	---	1-5/16	---	Run terminated. Boule hitting gas tube. Too large.
-26	$\langle 001 \rangle$	3/4 x 3/4	2-7/16	1/8" Conical	Golden yellow. Good except second phase inclusions last 1/4".
-27	$\langle 100 \rangle$	1/2 x 3/4	2-1/8	1/8" Conical	Two twins started at first shoulder, but major crystal is good color and quality.

## IV. APPLIED DESIGN OF YVO<sub>4</sub> POLARIZING DEVICES

### A. INTRODUCTION

A thorough analysis has been carried out for YVO<sub>4</sub> as it would be used in conventional polarizing devices. This analysis is presented in detail in Part IV-F. It considers the direct substitution of YVO<sub>4</sub> for calcite and demonstrates the improved performance which can be anticipated over a full range of wavelengths. In this section, we will use the results of the more general analysis and apply them specifically towards prisms operating at 1.06 microns. Thus we can study the material and the polarizer performance relative to the requirements for Nd:YAG rangefinders.

Two main polarizers are currently used inside a solid state Nd:YAG laser cavity in conjunction with the electrooptic Q-switch. These are the Glan polarizer and the Rochon polarizer-beam splitter. Both of these devices produce an undeviated polarized beam. The Glan-type polarizer has the added advantage that it removes one ray completely and thus avoids the complications that arise with the Rochon prism's deviated ray being reflected within the cavity. Each polarizer is described and advantages derived from the substitution of YVO<sub>4</sub> for calcite are delineated.

The most serious problem associated with single crystal polarizers when they are used in laser systems is the energy loss which the beam suffers in passing through the device. These losses arise from a number of sources, and an indication of their importance is seen when it is considered that a 1% loss in the polarizer can account for about an 8% loss in the overall laser output. The main sources of energy loss which are common to both the Glan and Rochon polarizers are:

- a. Scattering and/or absorption due to poor internal quality.
- b. Surface reflection and scattering losses. This is a combination of Fresnel losses and surface finish effects.
- c. Reflection losses resulting from the passage of the ray from one prism to the next.

- d. Inadequate dimensional stability and poor alignment of the prisms relative to each other.

Each of the above factors will be considered below and the anticipated performance of  $\text{YVO}_4$  polarizers discussed relative to similar devices fabricated from calcite.

## B. MATERIAL QUALITY

With the exception of quartz, all laser-quality synthetic materials are grown from a stoichiometric melt. This method has consistently shown itself capable of producing the finest quality material necessary for high performance laser systems; it has decisively beaten out competition from the hydrothermal and flux techniques. Stoichiometric  $\text{YVO}_4$  can be grown from a melt and thus can realize an optical quality equivalent to that of the laser itself and its system's electrooptic components.

## C. SURFACE REFLECTION AND SCATTERING LOSSES

Because of its low hardness, calcite, in its final polished form, possesses a surface quality which is not equal to that normally demanded for laser components. The finish is frequently not consistent over the whole aperture area, and sub-surface scratches remain which cause scattering and introduce serious loss problems.  $\text{YVO}_4$  has a hardness which is equivalent to most optical glasses permitting a wider choice of polishing abrasives and techniques. This higher hardness value then permits an improvement in overall fabricability, resulting in a superior surface finish. It also allows more precise control of the surface in terms of both flatness and the ability to effect parallelism. Thus, a more reproducible fabrication process with improved potential for mass-production operation can be anticipated.

Minimization of Fresnel losses for the polarizer requires good anti-reflection coatings on the entrance and exit faces. Because of the high refractive index for  $\text{YVO}_4$  (1.96 at 1.06 microns), good AR coatings can be achieved using the more common single-layer coatings rather than resorting to the multi-layer coatings which must be used with calcite. This property permits a more reproducible coating process to be used and an improvement by almost an order of magnitude in the coating cost.

#### D. REFLECTION LOSSES BETWEEN PRISMS

The situation regarding reflection losses differs for the Glan and Rochon designs and each is considered separately below:

##### a. GLAN POLARIZER

In this design, an air gap is maintained between the fabricated prisms and losses occur through multiple reflections within this gap. Detailed calculations for these energy losses have been made in Part IV-F using both  $\text{YVO}_4$  and calcite as the doubly refracting material. For optimum performance,  $\text{YVO}_4$  (a positive uniaxial material) requires a Glan-Foucault design, whereas for calcite (a negative uniaxial material) a Glan-Taylor design is required.<sup>13</sup>

These calculations further show that a combination of high refractive index and larger birefringence reduces the reflection losses in the air gap to 0.9% for  $\text{YVO}_4$ . This compares to calcite losses at 5.2%. The comparison is made using prism angles of  $27.5^\circ$  and  $28.5^\circ$  for  $\text{YVO}_4$  and calcite, respectively. The lower limit for calcite can be found by decreasing the prism angle to  $37.5^\circ$  which is the critical angle at 1.06 microns; this design change only serves to decrease losses to about 3%. Thus, the advantages of  $\text{YVO}_4$  over calcite in decreasing the losses in this critical area of the polarizer can be clearly seen.

##### b. ROCHON POLARIZER

For the design of the Rochon, the prisms are "welded" together in intimate contact. This requires either a suitable cement with index matching properties or, ideally, optical contacting. Assuming perfect optical contacting, calculations have been made in Part IV-F showing the degree of beam splitting achieved through the use of both  $\text{YVO}_4$  and calcite. Again it can be seen that the combined increase in refractive index and birefringence allows a 30% increase in the beam splitting capabilities of  $\text{YVO}_4$  over calcite.

Because of the problems associated with absorption in even the best bonding cement layer between prisms, it is preferable to effect optical contacting, if at all possible, for ideal polarizer performance. Again, due to the hardness/fabrication problems of calcite, the latter situation is almost impossible to achieve. Our experience to date with the fabrication of  $\text{YVO}_4$  would indicate very strongly that the type of

surfaces and dimensional stability required for optical contacting will be possible. Thus the Rochon design can be utilized to its full advantage with the losses experienced by the passage of light through the prism faces kept to a minimum.

The material properties required to obtain optical contacting for the Rochon can also be utilized to good advantage in maintaining the flatness and parallelism required for the matching faces of the prism in the Glan polarizer. The calculations assumed perfect surfaces; any deviation from this condition could increase the ideal loss figure.

#### **E. DIMENSIONAL STABILITY AND PRISM ALIGNMENT**

Maintaining good stability of the polarizer dimensions and effecting precise alignment of the prisms for temperature variations up to a span of 70°C is one of the more critical problems of current polarizer designs used in military systems having environmental specifications. Any movement of the prisms from the set position would misalign the beam and drastically reduce the laser output. The problem is largely a mechanical one, and its solution lies in the use of a more satisfactory design of the holder for the polarizer device. The higher hardness and the reduced tendency for  $\text{YVO}_4$  to cleave or fracture under mechanical stress implies that a holder can be designed using a firmer grasp of the device and restrain mechanical movement during operational temperature fluctuations.

## F. POLARIZING DEVICES OF THE DOUBLE-REFRACTION TYPE

### 1. SUMMARY OF EXISTING POLARIZER DESIGNS

A number of polarizing devices are in general use which take advantage of the properties of doubly refracting mineral crystals. The most famous is the Nicol prism which was invented in 1828. This device utilizes optically clear calcite in the natural rhombic form which is cut along a diagonal and cemented together again with Canada balsam. In operation the ordinary ray is reflected, the extraordinary ray is transmitted. This device has been superseded by the Glan type polarizer and will not be described in any detail. Its main attribute lay in the fact that naturally cleaved rhombohedral crystals could be used and thus allow full utilization of the available good quality calcite. Two drawbacks to the design are lateral displacement of the beam, and astigmatism due to the oblique entrance and exit faces.

More attractive and currently more useful devices are the Glan polarizers. These generally are of two types, the Glan-Thompson and Glan-Foucault polarizers where the prisms are separated by cement or air, respectively. These Glan-type polarizers are the most widely used in laser systems and will be analyzed with special reference to  $\text{YVO}_4$  as the doubly refracting material.

Of particular interest to the laser industry is the combination of a polarizer and a beam splitter. These are constructed in the form of either a Rochon or a Wollaston Prism. These prisms will be further described and analyzed with specific reference to  $\text{YVO}_4$  as the polarizer material.

### 2. GLAN-TYPE POLARIZERS

The Glan-Foucault type polarizer represents the most useful current design and is constructed from two pieces of doubly-refracting material, each in the form of a right angle prism. The two pieces are cut so that the geometrical axis of the prism is parallel to the optic axis and placed together with a thin air gap between the respective hypotenuse faces; this is shown in Figure 4-1.

An analysis will be made for the Glan-Foucault polarizer, and its predicted performance, utilizing  $\text{YVO}_4$ , will be compared with similar

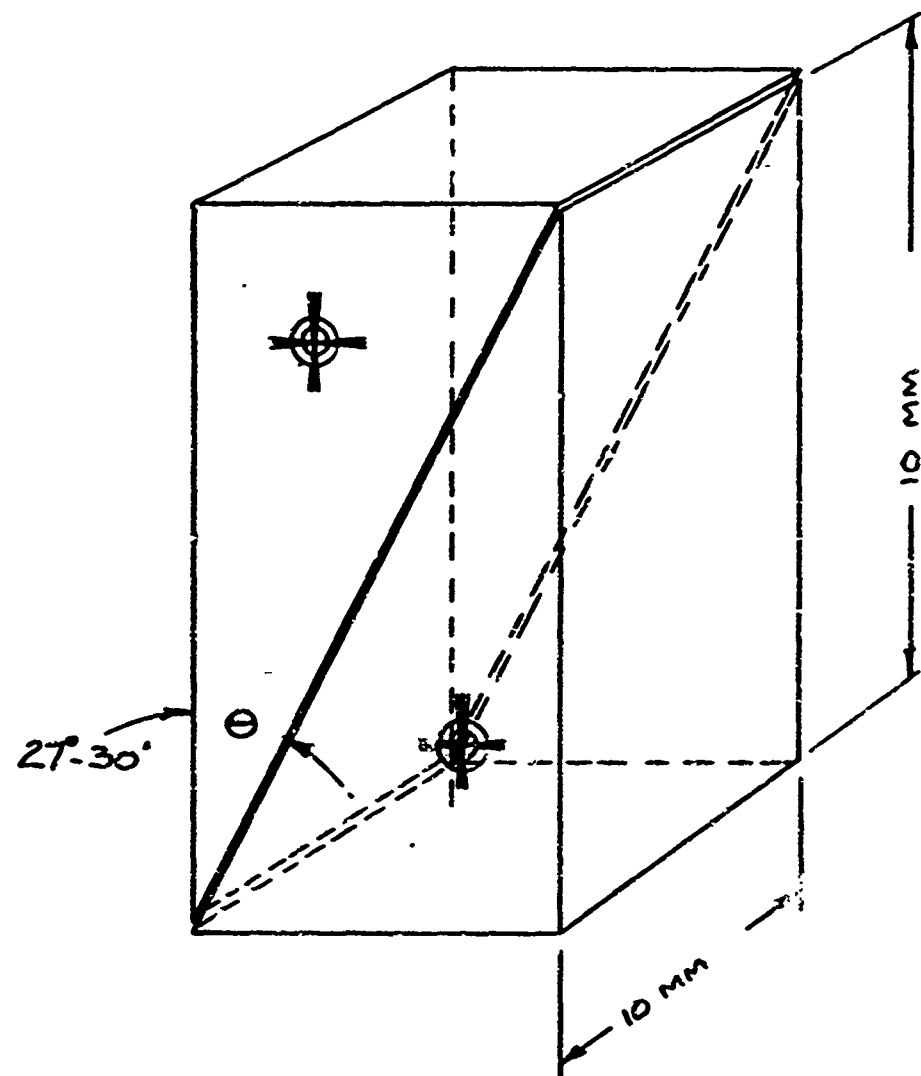


Figure 4-1. Glaß-Foucault Polarizer

devices made from calcite. Polarizers have been fabricated from good quality  $\text{YVO}_4$  single crystals, and measured performance will be discussed.

## a. ANALYSIS OF $\text{YVO}_4$ GLAN-FOUCAULT POLARIZER

Both the polarizer design and the choice of angle  $\theta$  for the prism is strongly dependent on the material used and the variation of refractive index of both the ordinary and extraordinary ray. Using Figure 4-2, where the critical angle is plotted as a function of wavelength for  $\text{YVO}_4$ , it can be seen that the most useful angle for a prism to operate in the visible and near infrared spectral region is  $27^\circ 31'$ . To extend the usefulness of this polarizer into the ultraviolet region requires a smaller angle of around  $27^\circ$  or slightly below.

Following Archard and Taylor,<sup>13</sup> the critical angles used in Figure 4-3 are calculated for an isotropic medium as this approximation introduces only small errors in the order of a few minutes. It should also be noted that, because we are dealing with a positive uniaxial material, the ordinary ray is transmitted and the extraordinary ray suffers total internal reflection.

A problem with the Glan polarizer design arises from the fact that multiple reflection occurs at the polished prism faces within the air gap. These reflections interfere with the performance of the polarizer for high intensity laser radiation and should be kept at a minimum; to do this requires an understanding of the losses experienced by polarized rays passing through the prisms.

The Fresnel formulae for reflectivity of polarized rays passing from one dielectric medium to another can be written:

$$R_{\parallel} = \frac{\tan^2(\theta_i - \theta_t)}{\tan^2(\theta_i + \theta_t)}$$

$$R_{\perp} = \frac{\sin^2(\theta_i - \theta_t)}{\sin^2(\theta_i + \theta_t)}$$

where  $R_{\parallel}$  and  $R_{\perp}$  are the reflectivity of rays polarized parallel and normal to the incidence plane; the incidence plane is defined as the plane

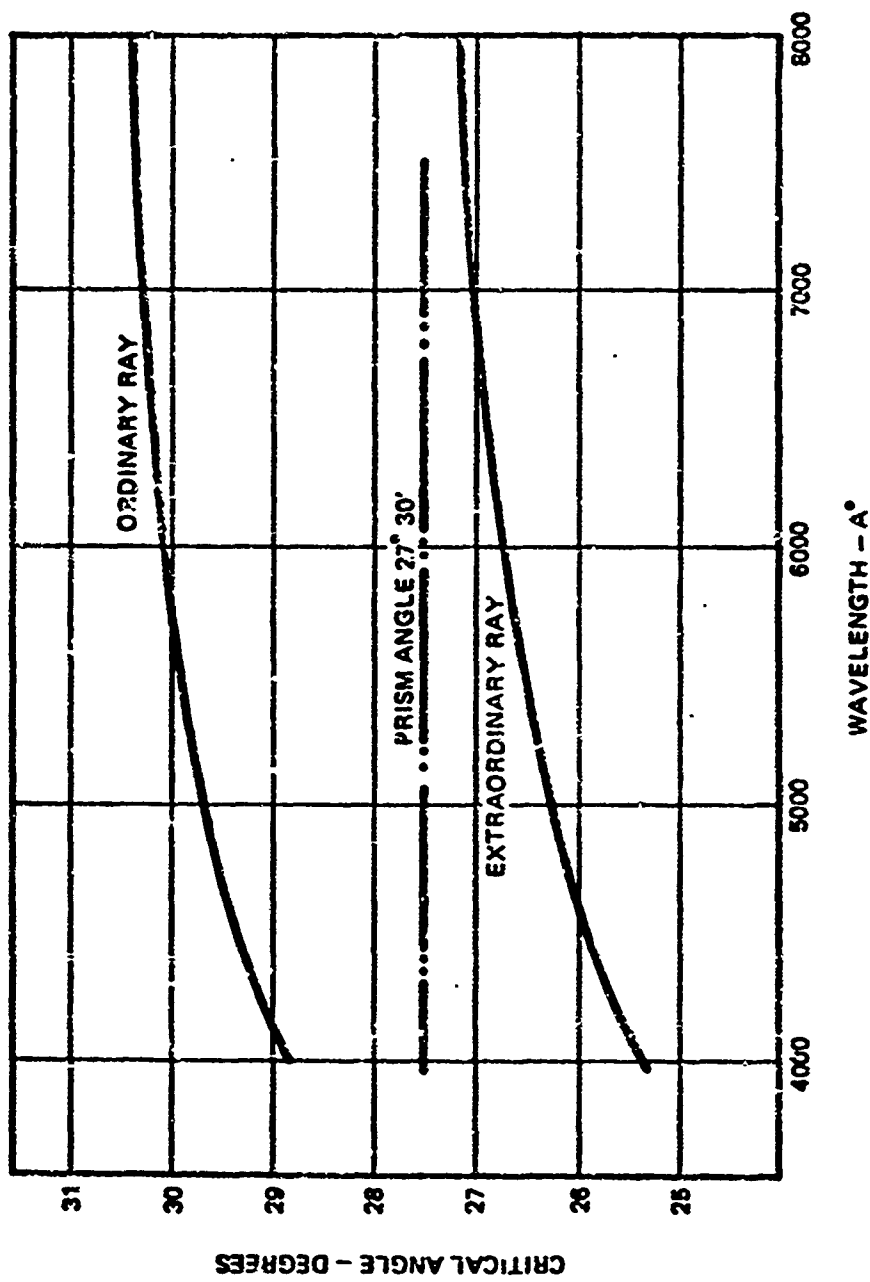


Figure 4-2. Critical Angle as a Function of Wavelength for  $\text{YVO}_4$

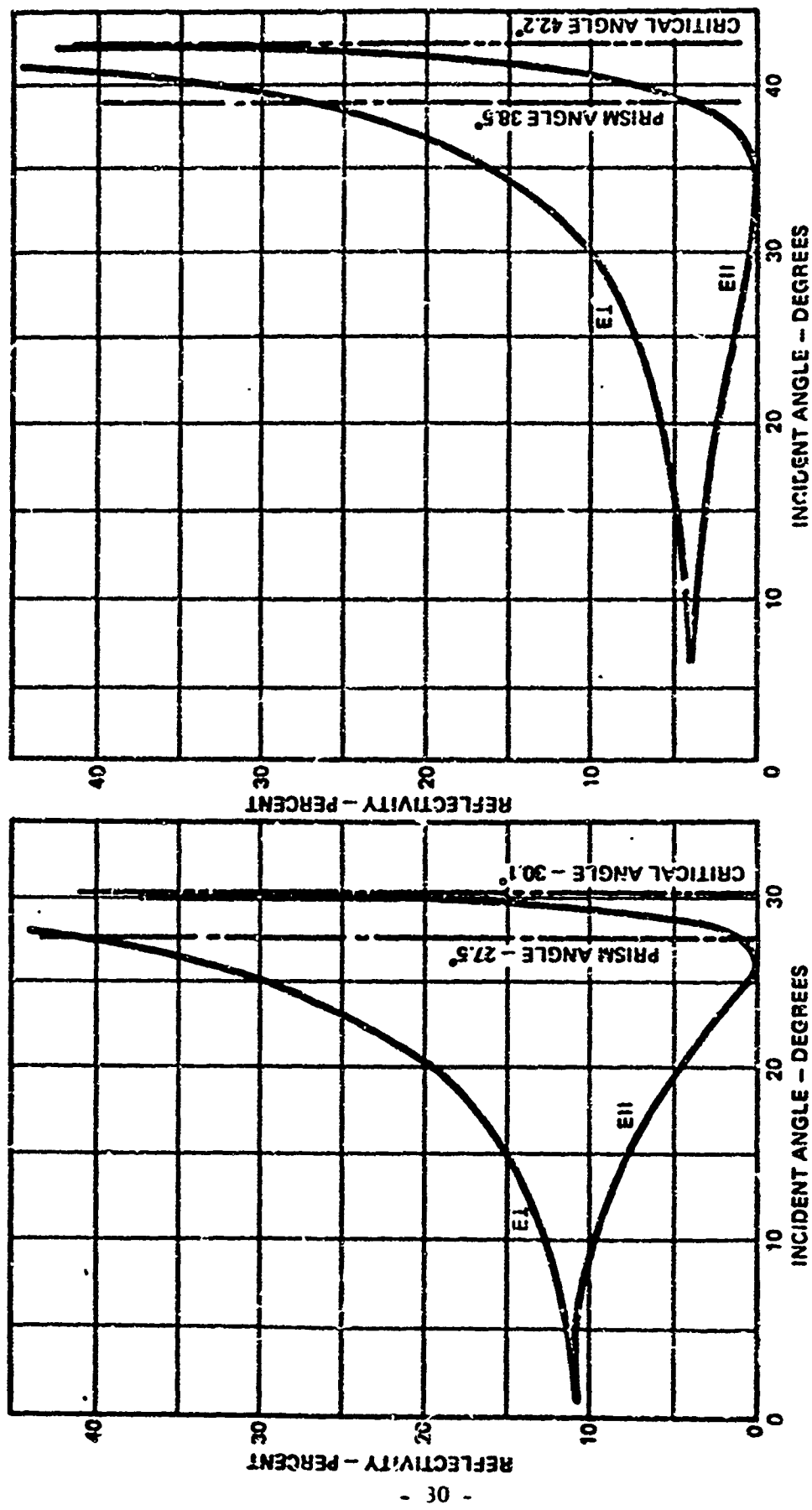


Figure 4-3. Reflectivity as a Function of Incident Angle for YVO<sub>4</sub>  
 Figure 4-4. Reflectivity as a Function of Incident Angle for Calcite

containing both the wave propagation direction vector and the normal to the boundary plane. The polarization direction of the ordinary and extraordinary rays is dependent on the direction of the optic axis relative to the wave normal direction. Thus, for a prism cut with the optic axis parallel to the intersection of the planes of the air film and end face (see Figure 4-5) the ordinary and extraordinary rays have their direction of polarization parallel and perpendicular to the plane of incidence at the air film.

Figure 4-3 and Figure 4-4 show the reflectivity, calculated from the Fresnel formulae plotted as a function of incidence angle for both  $\text{YVO}_4$  and calcite using a wavelength of  $6000\text{\AA}$ ;  $E_{\parallel}$  and  $E_{\perp}$  refer to the extraordinary and ordinary rays in the Glan-Foucault prism. It can be seen from the figures that minimum reflection occurs when the transmitted light is polarized parallel to the incidence plane at the air film.

$\text{YVO}_4$  being a positive uniaxial crystal, it is the ordinary ray which is transmitted and the Glan-Foucault design is the correct one for maximum transmission. For calcite using the same design it is the extraordinary ray which is transmitted with  $E$  perpendicular to the incidence plane; this represents an undesirably high reflectivity. The problem can be solved by cutting the first prism so that the optic axis is perpendicular to the intersection of the planes of the end face and the air film. This design turns the electric vector of the transmitted component to be parallel to the incidence plane, and is known as the Glan-Taylor prism.<sup>13</sup>

Calculations have been made showing the total transmitted energy through both the air gap and the second prism as a fraction of the energy in the first prism; these are represented by  $T'$  and  $T_1$  in Figure 4-5. The reflected energies  $R_1$  and  $R_2$  within the air gap are also calculated along with the energy  $T_2$  of the second transmitted ray; again these are given relative to a transmitted energy of unity in the first prism.

The results of these calculations are shown in Table IV-1 where a comparison is made between  $\text{YVO}_4$  cut with a Glan-Foucault polarizer design, and calcite cut with both a Glan-Foucault and a Glan-Taylor design. The wavelength used in all cases was  $5393\text{\AA}$ . The  $\text{YVO}_4$  had a prism angle of  $27.5^\circ$  and calcite an angle of  $38.5^\circ$ ; these angles are optimum for both materials.

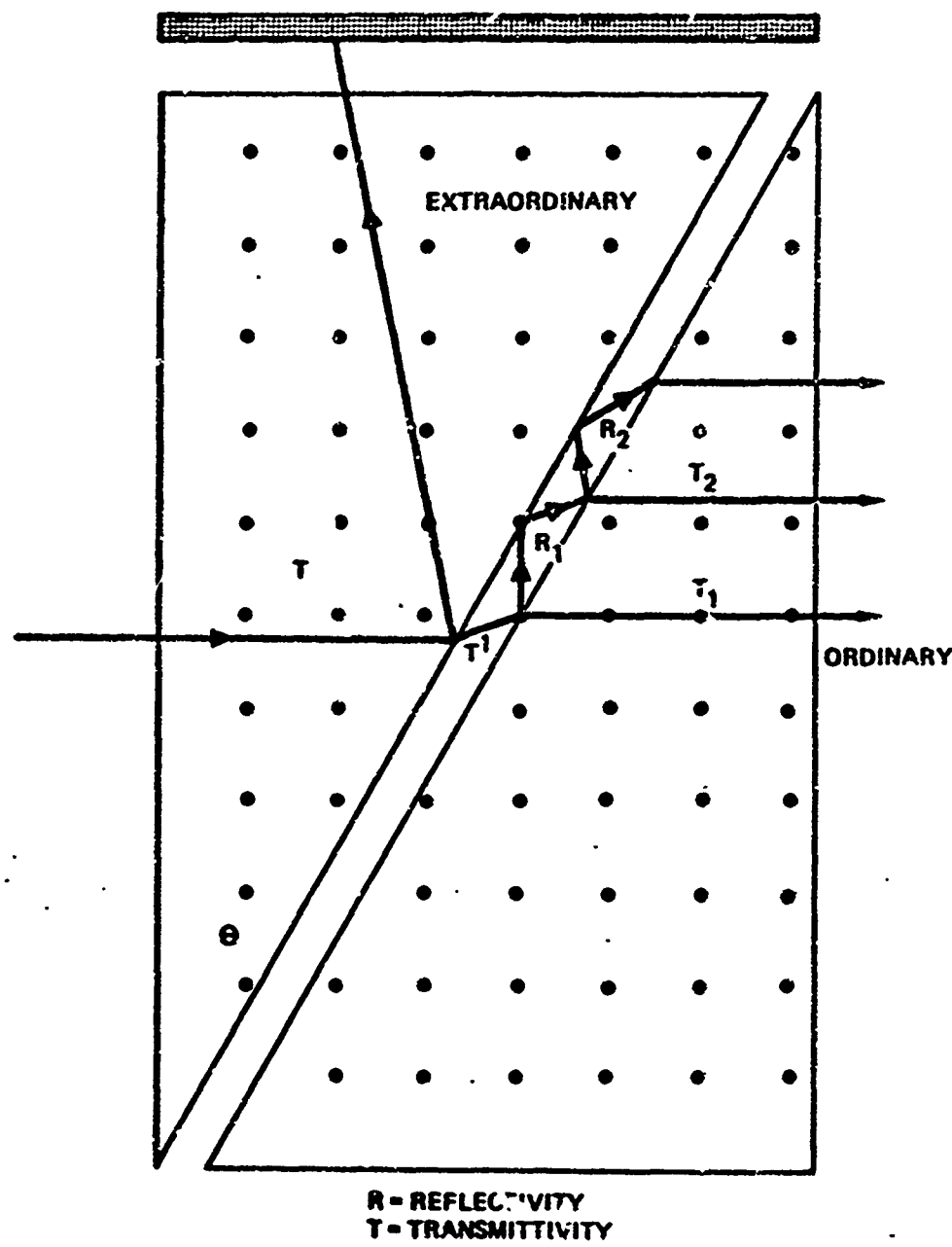


Figure 4-5. Glan-Foucault Polarizer Design Schematic. As shown above, ordinary ray is transmitted for  $\text{YVO}_4$  which has a positive sign of birefringence. For calcite, with a negative sign of birefringence, the extraordinary ray is transmitted.

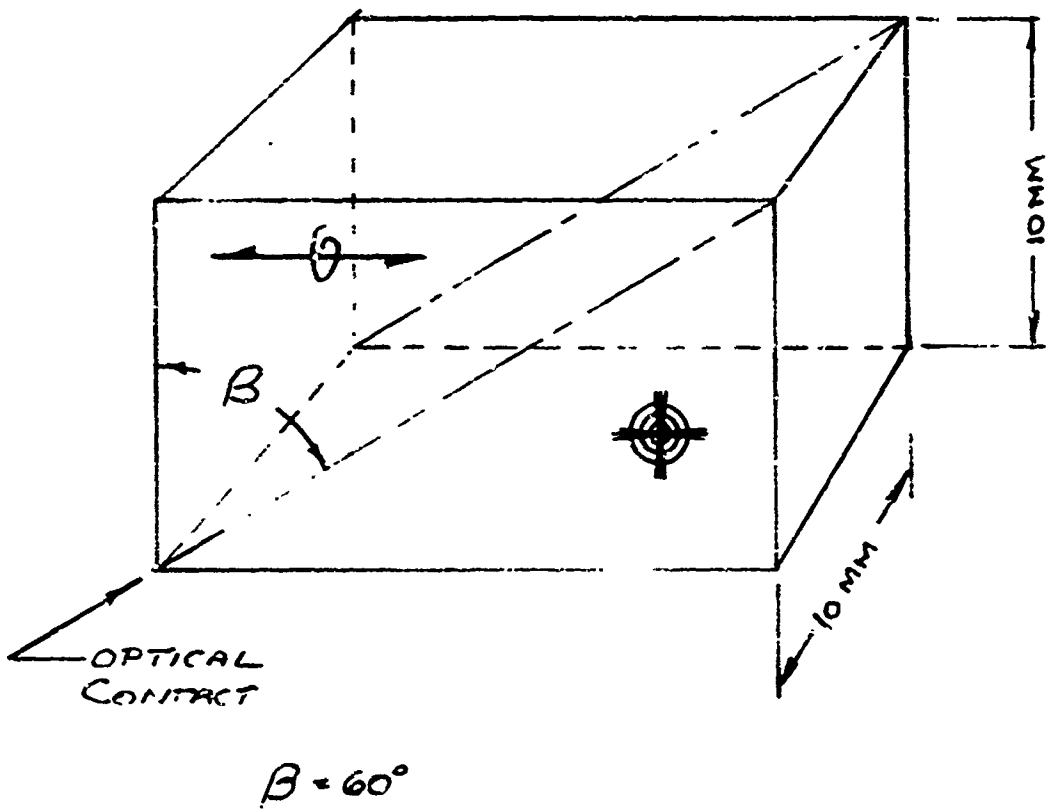


Figure 4-6. Rochon Polarizer Design

Prism	Material	Prism Angle	Ray N	T	T <sup>1</sup>	T <sub>1</sub>	R <sub>1</sub>	R <sub>2</sub>
Gian-Foucault	YVO <sub>4</sub>	27.5	Ord. 1.9974	1.000	0.995	0.991	0.005	10 <sup>-5</sup>
Gian-Taylor	Calcite	38.5	Extr. 1.486	1.000	0.974	0.948	0.026	0.001
Gian-Foucault	Calcite	38.5	Extr. 1.486	1.000	0.742	0.933	0.258	0.066

Table IV-1. The Relative Intensities of Transmitted and Reflected Rays Within the Air Gap for Different Prism Designs.

It should be noted that the vanadate prism gives the best performance with 99.9% of the polarized incident energy being transmitted in the main beam, with a reduction of  $10^{-5}$  for the secondary beam. Equivalent figures using calcite are 97.4% and 74.2% for the main beam, and  $10^{-3}$  and  $10^{-1}$  for the secondary beam. Changing from the Glan-Foucault to Glan-Taylor design reduces the intensity of the secondary transmitted beam by two orders of magnitude. A similar reduction is realized by going from the best calcite design to a Glan-Foucault prism using yttrium vanadate.

This improved performance becomes more important for high power laser use when it is considered that the input beam can have power levels up to  $10^6$  watts. The reduction by two orders of magnitude will allow the polarizer to be used under high power conditions which are currently unattainable with calcite prisms.

#### b. PERFORMANCE OF FABRICATED POLARIZER

Glan-Foucault polarizers have been fabricated to Figure 4-1 dimensions from boule #SD218-22-9 shown in Figure 4-7. The upper photograph shows the Twyman-Green presentation of the crystal with the photographic plane normal to the 001 axis. Figure 4-8 is the Schlieren image of the Glan-Foucault polarizer and Figure 4-9 shows the effect of  $90^\circ$ ,  $45^\circ$  and crossed polars on the polarizer.

Unpolarized light from a He-Ne gas laser of  $6328\text{\AA}$  wavelength was passed into the polarizer at normal incidence. This ray was split into the ordinary and extraordinary components and emerged from the exit face of the polarizer. The angle of separation was measured for the Rochon operational mode and found to be  $21^\circ$ .

There is excellent agreement between the calculated and experimentally measured values for the angular separation of the polarizers, demonstrating conclusively that  $\text{YVO}_4$  is a superior material over calcite for this application. The Rochon deviator showed a five degree improvement over calcite with similar dimensions. For a Wollaston device fabricated with a prism angle of  $60^\circ$  this improvement would be over ten degrees and an angular separation of  $42^\circ$  would be anticipated.

Using a high quality calcite polarizer of Glan-Taylor design the following experiments were carried out:

(1) Light from a He-Ne laser was passed through the calcite polarizer and the power measured on a well calibrated Spectra-Physics power meter.

(2) The  $\text{YVO}_4$  polarizer was then placed between the calcite polarizer and the meter in the parallel position and the overall transmission loss recorded. This overall loss was measured at 25%.

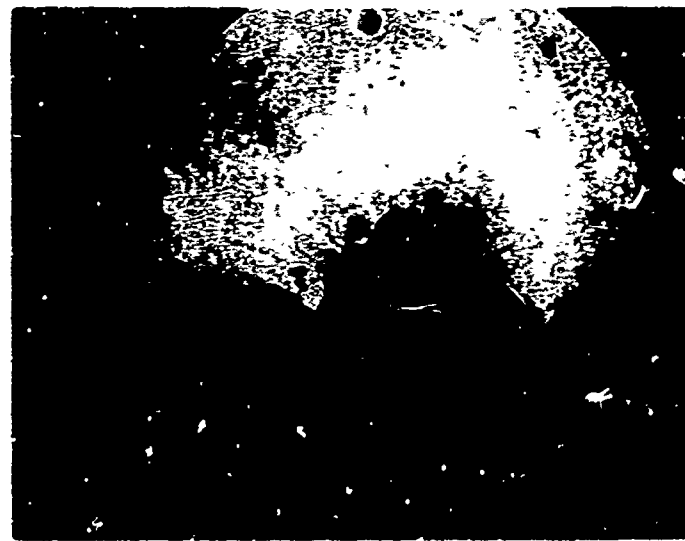


**Figure 4-7.  $\langle 001 \rangle$  YVO<sub>4</sub> Boule  
For Glan-Foucault Prisms**

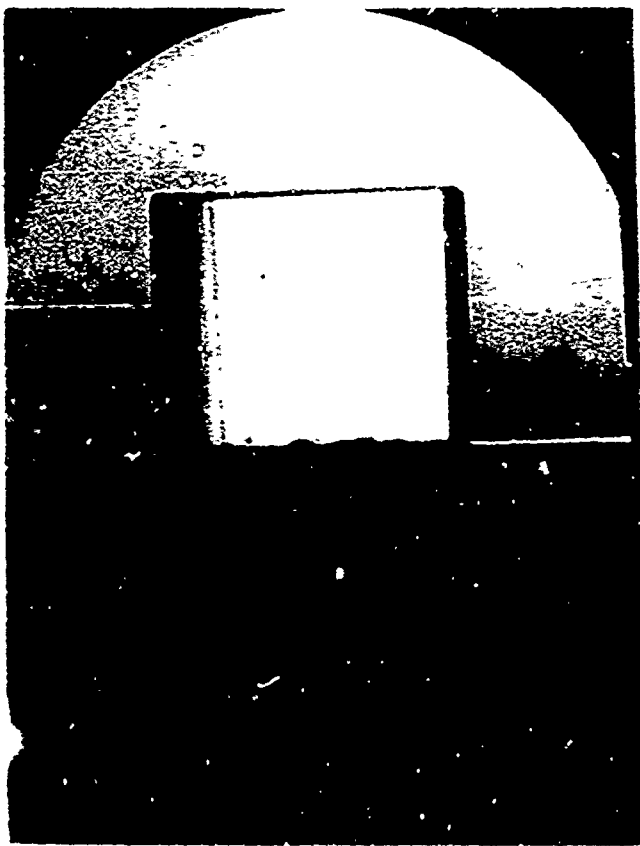
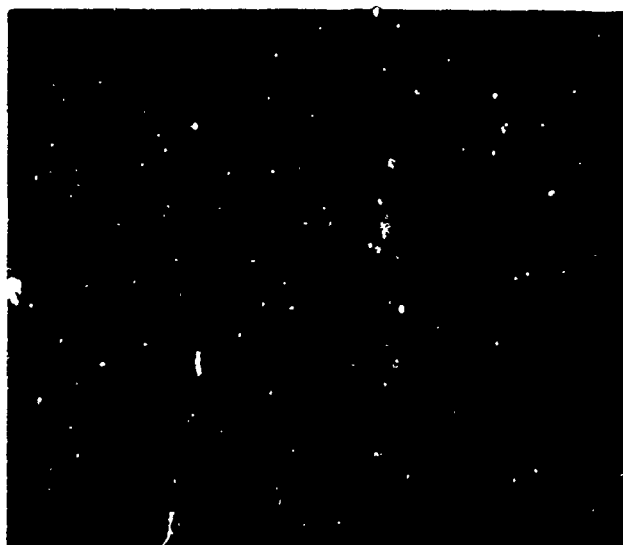
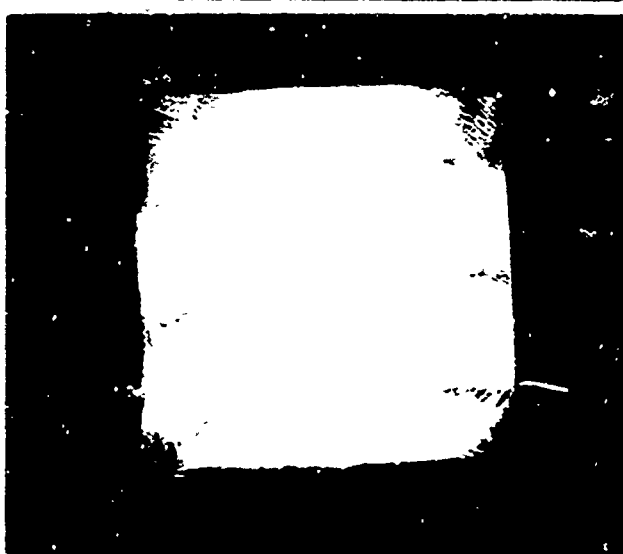


**Figure 4-8. Schlieren Image Through  
Glan-Foucault Polarizer**



0/90° Polars  
1/10" 3000 ASA



+ 45° Polars  
1/25" 400 ASA



X CIR Polars  
1/25" 400 ASA

Figure 4-9. Crossed Polar Photographs  
Through Glan-Foucault Polarizer

which allowing for an 11% loss at the entrance and exit face due to Fresnel reflection, gave a combined material and "air gap" loss of 3%.

(3) The  $\text{YVO}_4$  polarizer was next rotated through 90 degrees into the crossed position and the power meter replaced by a photomultiplier. The transmitted light was outside the detection limit of the measuring equipment and an accurate value for transmission, which translates to an extinction ratio of greater than 35 decibels.

### 3. ROCHON AND WOLLASTON POLARIZERS

#### a. INTRODUCTION

These polarizers differ from the Glan-type insofar as they preserve both of the refracted beams, but separate them widely enough to be used individually. They are both polarizers and polarizing beam splitters. The makeup of the polarizer is shown in Figure 4-6 where two right angle prisms are cut from a suitable doubly refracting material, and optically contacted together. The optic axes of the two prisms are mutually perpendicular. In the description of the emerging beams and their direction of polarization, a positive uniaxial crystal is assumed for the illustration.

Again, these polarizers will be analyzed with special reference to  $\text{YVO}_4$  as the doubly refracting material and their performance projected relative to calcite. The analytical results will then be compared directly with a fabricated polarizer.

#### b. ANALYSIS OF $\text{YVO}_4$ ROCHON POLARIZER

With the Rochon polarizer, the unpolarized incident ray travels along the optic axis and is split up into two rays each with the same velocity. On transferring across the prism interface, the ordinary ray maintains the same velocity and proceeds through the second crystal undeflected. The velocity is changed for the extraordinary ray and it is deflected. Further separation occurs when the extraordinary ray leaves the second prism, and the angle of divergence can be calculated using standard optical techniques.

To demonstrate the strong influence of the birefringence we have represented the divergence angle through the following approximate formula:

$$\sin \theta = \frac{(n_E - n_O) \sin 2B}{2} \quad 1 + \frac{(n_E + n_O) \tan^2 B}{2n_E}$$

where  $B$  is the prism angle, and  $n_E$  and  $n_O$  are the refractive indices for the extraordinary and ordinary rays.

The divergence angle  $\theta$  has been calculated also and shown in Table IV-2 as a function of prism angle  $B$  for different wavelengths using yttrium vanadate, calcite, and quartz as the prism materials; this was a computer calculation using the more rigorous derivation, and assuming perfect optical contacting between the prism faces. As can be seen, a significant improvement is projected for the divergence angle  $\text{YVO}_4$  over both calcite and quartz.

#### c. ANALYSIS OF $\text{YVO}_4$ WOLLASTON POLARIZER

For the Wollaston polarizer, the direction of the optic axis is changed for the first prism and an unpolarized incident ray is split up into two polarized beams each travelling in the same direction with different velocities determined by the corresponding refractive indices for each beam. On transferring across the prism interface, the ordinary ray in the first prism becomes the extraordinary ray in the second; the extraordinary ray is converted to the ordinary in a similar fashion. The resulting refractive index change causes the two polarized beams to be deflected at the interface. Further separation occurs when the beam passes from the high index crystal into air. The divergence angle for the Wollaston polarizer is approximately twice that realized for the Rochon polarizer. It does, however, suffer from the disadvantage that both transmitted beams are divergent. Values for the divergence angles for a  $\text{YVO}_4$  Wollaston polarizer as a function of prism angle would be double those shown in Table IV-2.

#### d. CONCLUSIONS OF ANALYSIS

It can be seen from the above calculations that  $\text{YVO}_4$  offers a substantial advantage in both the Rochon and Wollaston design over calcite and quartz. For a prism angle of  $60^\circ$  and assuming perfect optical contacting, the divergent angle for  $6500\text{\AA}$  is increased by over 30% when  $\text{YVO}_4$  is substituted for calcite. This factor is even more significant when it is considered that the improved fabricability of the orthovanadate makes optical contacting a much easier proposition.

#### e. PERFORMANCE OF THE ROCHON POLARIZER

A Rochon polarizer was fabricated from <100> boule No. SD218-18-7. The boule and its Twyman-Green pattern are shown in Figure 4-10 and the construction design is shown in Figure 4-6. The two prisms were contacted with Opticon UV-57 cement having a refractive index of 1.5316 and good transmission to 2 micron wavelength.

Material	Prism Angle						Wave-length A
	25	30	35	40	45	50	
$\gamma\text{VO}_4$	5.98	7.37	8.88	10.56	12.44	14.60	17.13
$\text{YVO}_4$	5.88	7.25	8.73	10.38	12.23	14.36	16.85
$\text{CaCO}_3$	4.50	5.54	6.67	7.93	9.33	10.94	12.80
Quartz	0.24	0.30	0.36	0.44	0.52	0.62	0.74
							0.89
							1.10
							5893

Table IV-2. The Angle of Separation for Polarized Rays Emerging from a Rochon Polarizer Cut at Different Prism Angles  $\beta$ . All angles expressed in degrees and equivalent to  $\theta$  in Figure 8-4.

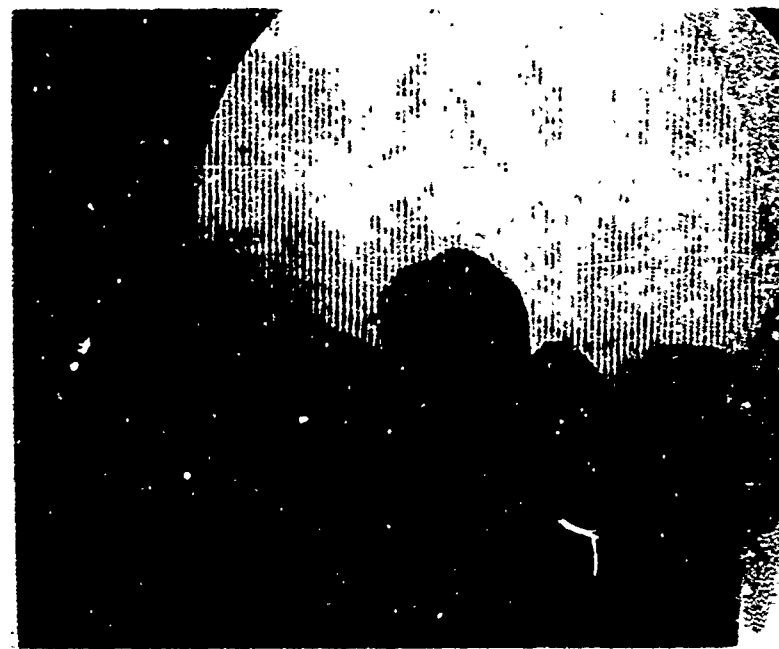


Figure 4-10.  $\langle 100 \rangle$  YVO<sub>4</sub> Boul. for Rochon Prisms

Unpolarized light from a He-Ne gas laser of  $6328\text{\AA}$ <sup>0</sup> wavelength was passed into the polarizer at normal incidence. This ray was split into the ordinary and extraordinary components and emerged from the exit face of the polarizer. The angle of separation was measured for the Rochon operational mode and found to be  $21^{\circ}$ .

There is excellent agreement between the calculated and experimentally measured values for the angular separation of the rays, demonstrating conclusively that  $\text{YVO}_4$  is a superior material over calcite for the Rochon polarizer. The fabricated Rochon polarizer showed a 5 degree improvement over a calcite polarizer with similar dimensions.

For a Wollaston polarizer of  $\text{YVO}_4$  with a prism angle of  $60^{\circ}$  this improvement would be over 10 degrees, and an angular separation of  $42^{\circ}$  would be anticipated.

## G. PRACTICAL CONSIDERATIONS FOR POLARIZER DESIGNS

### 1. INTRODUCTION

The discussions to this point on polarizers and polarizing materials have considered only the combined effect of refractive index and birefringence on the optical properties and the device performance. Other losses due to surface and internal scattering were assumed to be negligible in the analytical treatment used, although some extent of the problem was given in the transmission and extinction measurements made on the Glan-Foucault polarizer. These losses are always present in some form and depend on a combination of internal material quality, fabrication, and the choice of suitably matched dielectric anti-reflection coatings. As they can seriously influence the overall performance of the polarizer, it is important that they also be considered along with the measured optical properties with every effort made to minimize their effect.

### 2. FABRICATION

Successful fabrication of calcite presents a problem because of the hardness difference relative to the optic axis, and the tendency for the material to cleave along the rhombohedral planes. To achieve the necessary tolerances for surface flatness and uniformity of polish, requires extremely careful handling and finishing procedures which utilize predominantly hand-lapping. This involved fabrication procedure with its high labor cost contributes to the high cost of the finished polarizer.

The polished surface finish for YVO<sub>4</sub> is superior to that for calcite and can be achieved with much more ease. This improvement in optical workability can be traced to a hardness which is similar to glass, and, more important, a lesser tendency to cleave. Cleavage has been induced and occurs parallel to the <001> axis. It does not, however, present any problems in the prism fabrication.

There are two main advantages to be realized from the improved surface finish and ease of optical working:

a. The material lends itself more easily to automated fabrication processes and can be handled by procedures more closely related to those experienced in a mass production operation.

b. Optical contacting of the polished surfaces can be achieved. This situation is difficult to achieve for calcite and is the main reason why devices such as the Rochon and Wollaston polarizers, which rely on good optical contacting, are frequently constructed from quartz. In this case, the reduced birefringence is compensated by the superior optical surfaces.

### 3. ANTI-REFLECTION COATINGS

If a dielectric film with refractive index  $n_2$  is placed on the surface of a medium with refractive index  $n_3$ , then for the case of normal incidence  $R$ , the reflectivity can be written as:

$$R = \frac{n_1 n_3 - n_2^2}{n_1 n_3 + n_2^2}$$

for a thickness  $H = \frac{m\lambda_0}{4}$  ( $m = 0, 1, 2, 3, \dots$ )

Thus, for zero reflectivity,  $n_2 = \sqrt{n_3}$  where the initial medium is air and  $n_1 = 1.000$ .

This normal incidence case is true for both the Glan-Foucault and Rochon polarizers. In order to minimize reflective losses at the entry and exit faces, a dielectric coating with refractive index 1.414 is required with YVO<sub>4</sub> prisms. For calcite, utilizing the same design, a refractive index for the dielectric layer would be 1.219.

The most readily available material for anti-reflection coatings is magnesium fluoride with a refractive index of 1.38. As can be seen, this provides a reasonably good match for  $\text{YVO}_4$ , but is much too high for calcite. Finding a suitable anti-reflection coating for use with calcite has been a problem in the past with no current solution.

## V. PROPERTIES OF YTTRIUM ORTHOVANADATE

### A. OPTICAL PROPERTIES

The optical and physical properties of yttrium orthovanadate are summarized in Table I-1. These values apply to single crystals of undoped material which have been grown recently in our laboratory. The optical measurements were made in the laboratory of Professor L. De Shazer at the University of Southern California, Los Angeles. Other property measurements were made at Crystal Products Laboratories, San Diego.

#### 1. BIREFRINGENCE

Yttrium orthovanadate ( $\text{YVO}_4$ ) is a positive uniaxial crystal with a birefringence higher than that of calcite by 25%. Birefringence is defined as the difference between the extraordinary and ordinary refractive index. For a wavelength of  $5890\text{\AA}$  (sodium - D line) the measured birefringence of  $\text{YVO}_4$  is +0.226 compared to a value of -0.172 for calcite. These measurements correct previously published results<sup>1</sup> by others which have reported a birefringence of the wrong sign.

#### 2. DISPERSION

The refractive index as a function of wavelength given for  $\text{YVO}_4$  in Table V-2 can be numerically expressed in terms of the wavelength for both the ordinary and extraordinary ray through the formulae:

$$\text{Extraordinary: } n_e^2 = 1 + \frac{3.5996 \lambda^2}{(\lambda^2 - 3.1346)}$$

$$\text{Ordinary: } n_o^2 = 1 + \frac{2.7710 \lambda^2}{(\lambda^2 - 2.6336)}$$

where the wavelength  $\lambda$  is in units of  $10^{-3}\text{\AA}$ . These equations are particular cases of Sellmeier's equations for dispersion.

For Table I-1 the dispersion has been defined more simply as  $n_F - n_C$  where F and C indicate the wavelengths 4861 and  $6563\text{\AA}$ . The dispersions for the ordinary and extraordinary indices of  $\text{YVO}_4$  are 0.04 and 0.06 respectively. These values are higher than those reported for calcite and quartz, but still within the range to allow the  $\text{YVO}_4$  polarizers to be used in large bandwidth optical systems.

Wavelength Å	Refractive Index		Birefringence
	Ordinary	Extraordinary	
4000	2.0777	2.3402	0.2625
4500	2.0458	2.2932	0.2474
5000	2.0242	2.2618	0.2376
5500	2.0088	2.2396	0.2308
6000	1.9974	2.2233	0.2259
6500	1.9888	2.2109	0.2221
7000	1.9820	2.2013	0.2193
7500	1.9766	2.1936	0.2170
8000	1.9723	2.1875	0.2152

Table V-2. Refractive Index as a Function of Wavelength for Single Crystal  $\text{YVO}_4$

The thermal variation of the refractive index is small and is shown in Figure 5-1 over the temperature range from 4°K to 300°K for a wavelength of 5148 Å. The refractive-index temperature coefficient  $dn/dT$  is  $+3.9 \times 10^{-5}$  per degree centigrade at room temperature for both ordinary and extraordinary rays.

### 3. SPECTRAL ABSORPTION

The spectral absorption has been measured for a polished  $\text{YVO}_4$  single crystal and is shown in Figure 5-2. The linear absorption coefficient  $\alpha$  is defined in the usual way as the negative of the inverse of the path length multiplied by the natural logarithm of the transmission. The region between 6.5 and 3.0 microns was deleted to the figure as there was no absorption over that range. It can be seen that  $\text{YVO}_4$  is highly transmissive from 0.4 to 3.8 microns and is optically useful up to 5.0 microns. A piece of calcite measured in the same system became absorptive at 2.1 microns and was opaque at wavelengths greater than 3.1 microns. The published transmission data for quartz indicates that it also becomes absorptive at 2.2 microns.<sup>14</sup>

## B. PHYSICAL PROPERTIES

### 1. HARDNESS

Hardness measurements were carried out on a cleaved (100) surface of a  $\text{YVO}_4$  single crystal. A Carl Zeiss Microhardness Tester MHP was used, attached to a Zeiss Universal Microscope. With a 50 gm load the measured Knoop hardness numbers (KHN) are as follows, where zero degrees implies that the long diagonal of the rhombic diamond indenter was coincident with the [010] direction.

$$\begin{array}{ll} 0^\circ = 199.6 & 90^\circ = 549.0 \\ 45^\circ = 452.0 & 315^\circ = 406.5 \end{array}$$

The zero degree measurement was anomalously soft due to cleavage occurring on the (100) crystallographic plane which gave extended deformation of the indentation along that particular direction. Away from this direction there was some slight variation due to the crystalline anisotropy. The average hardness of 480 KHN is equivalent to most high quality optical glasses. It should be compared with a value of 135 KHN for calcite and 710 KHN for quartz.<sup>15</sup>

### 2. LASER DAMAGE RESISTANCE

To measure the laser damage resistance for  $\text{YVO}_4$  compared to calcite, the output from a Q-switched ruby laser was focused into polished single crystal rectangular pieces. After each firing the samples were inspected for damage by passing a He-Ne laser beam through

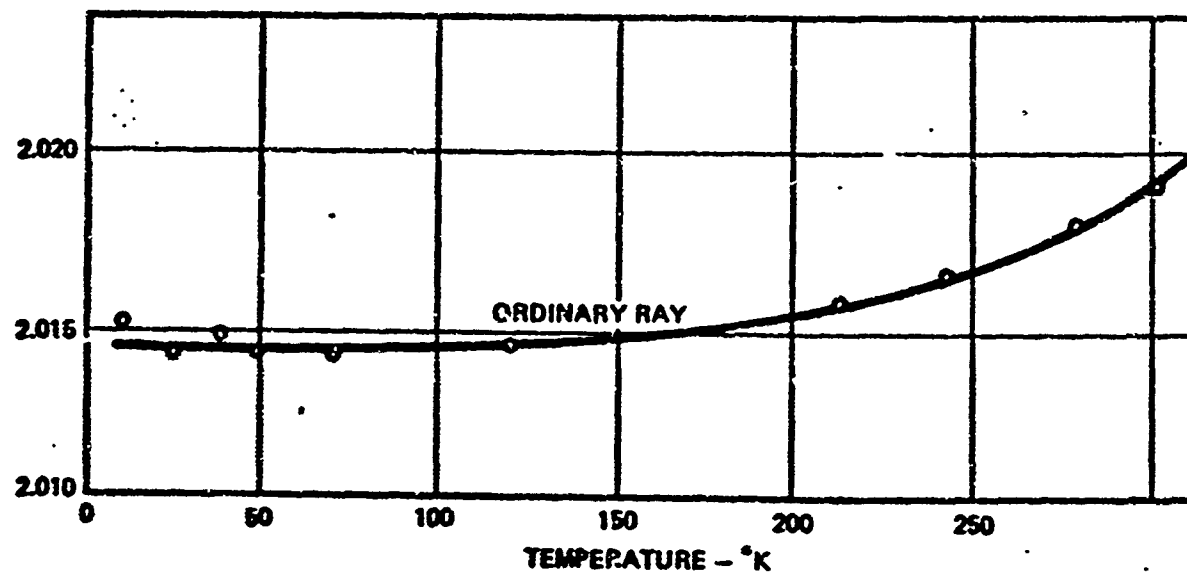
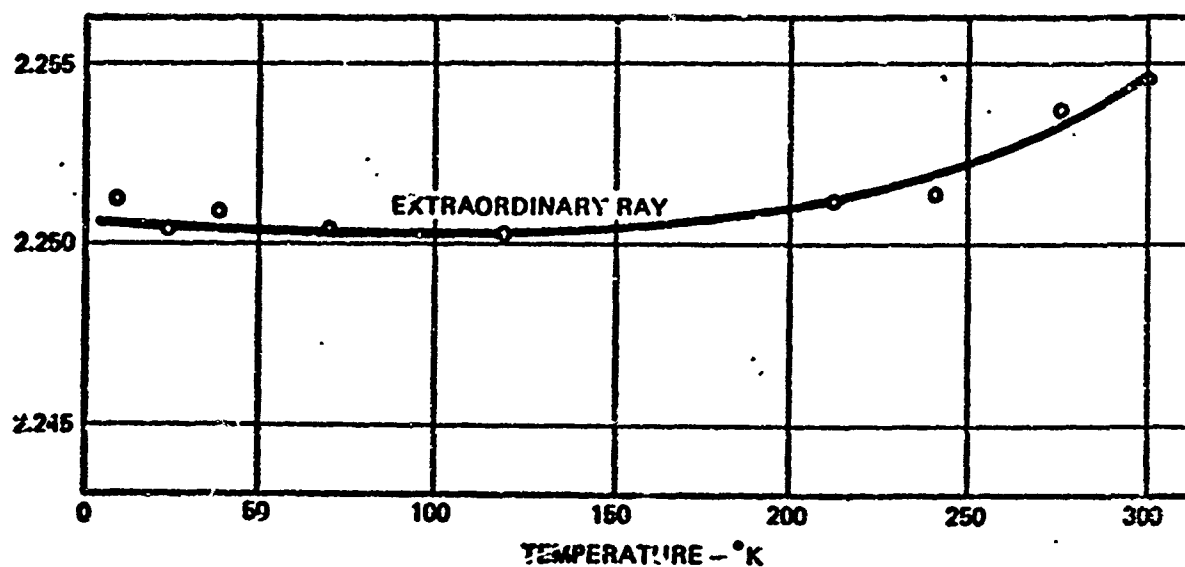


Figure 5-1. Change in Refractive Indices as a Function of Temperature for Single Crystal YVO<sub>4</sub>

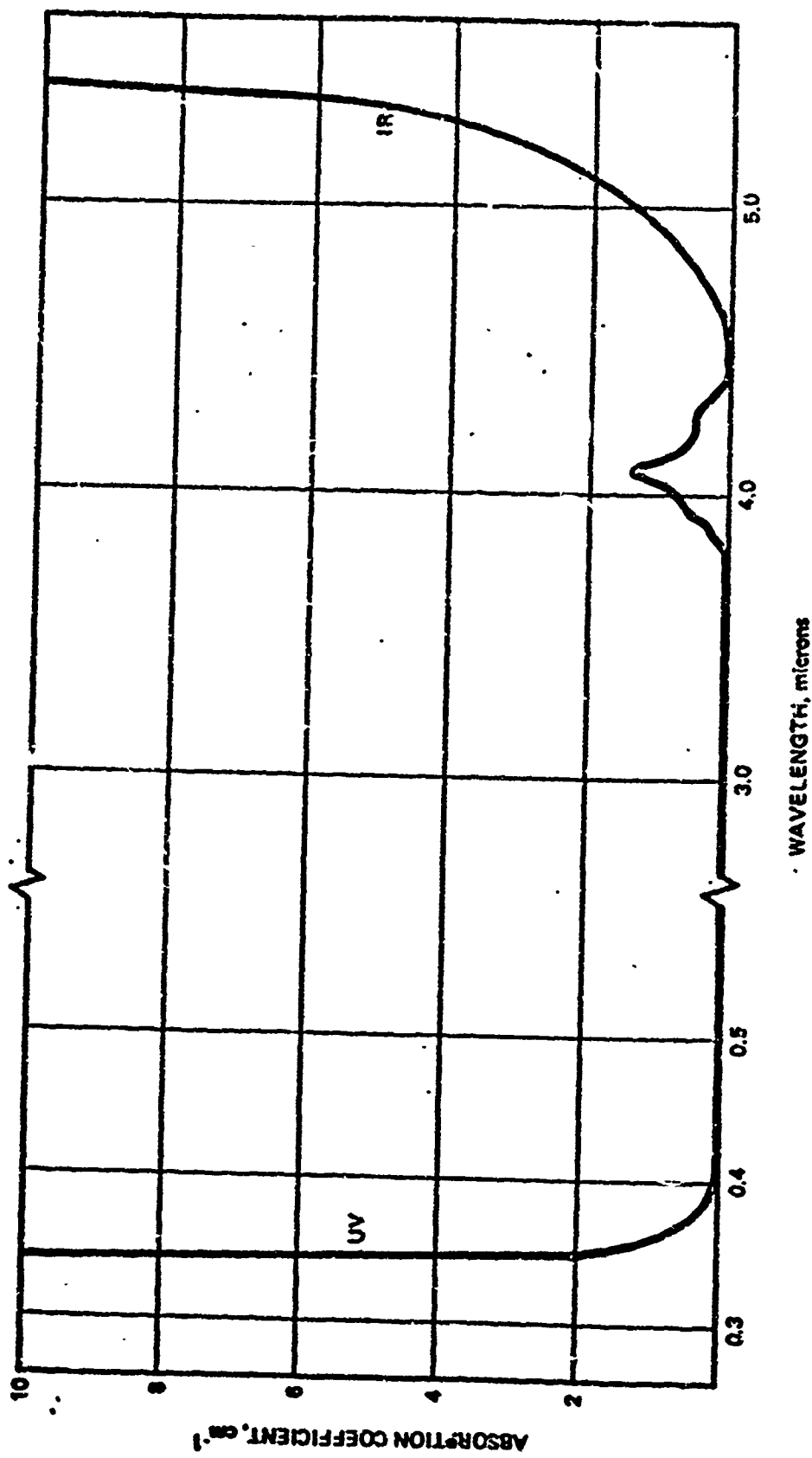


Figure 5-2. Absorption Coefficient for  $\text{TiVO}_4$  Plotted Versus Wavelength

the material and looking for scattering. The results are shown in Figure 5-3. Calcite started to damage at power levels in the range 900 to 1200 MW/cm<sup>2</sup> and suffered extensive damage for all levels tested above this range. In every case the damage was internal to the material and was gross enough to seriously affect the optical quality and overall device performance.

Single crystal YVO<sub>4</sub> prisms submitted to laser testing prior to this contract had shown some slight surface damage in the 900 to 1200 MW/cm<sup>2</sup> power range. This damage was noted only after testing to 2400 MW/cm<sup>2</sup> at which point surface damage was evident. No internal structural damage was noted at that time and the surface damage was estimated to be a function of the surface finish on the test sample.

A prism has been prepared from a crystal grown for this contract and has been submitted to laser damage study. Preliminary data, at gradually increasing power, has shown that the damage threshold has not yet been reached at 3 giga watts per cm<sup>2</sup>.

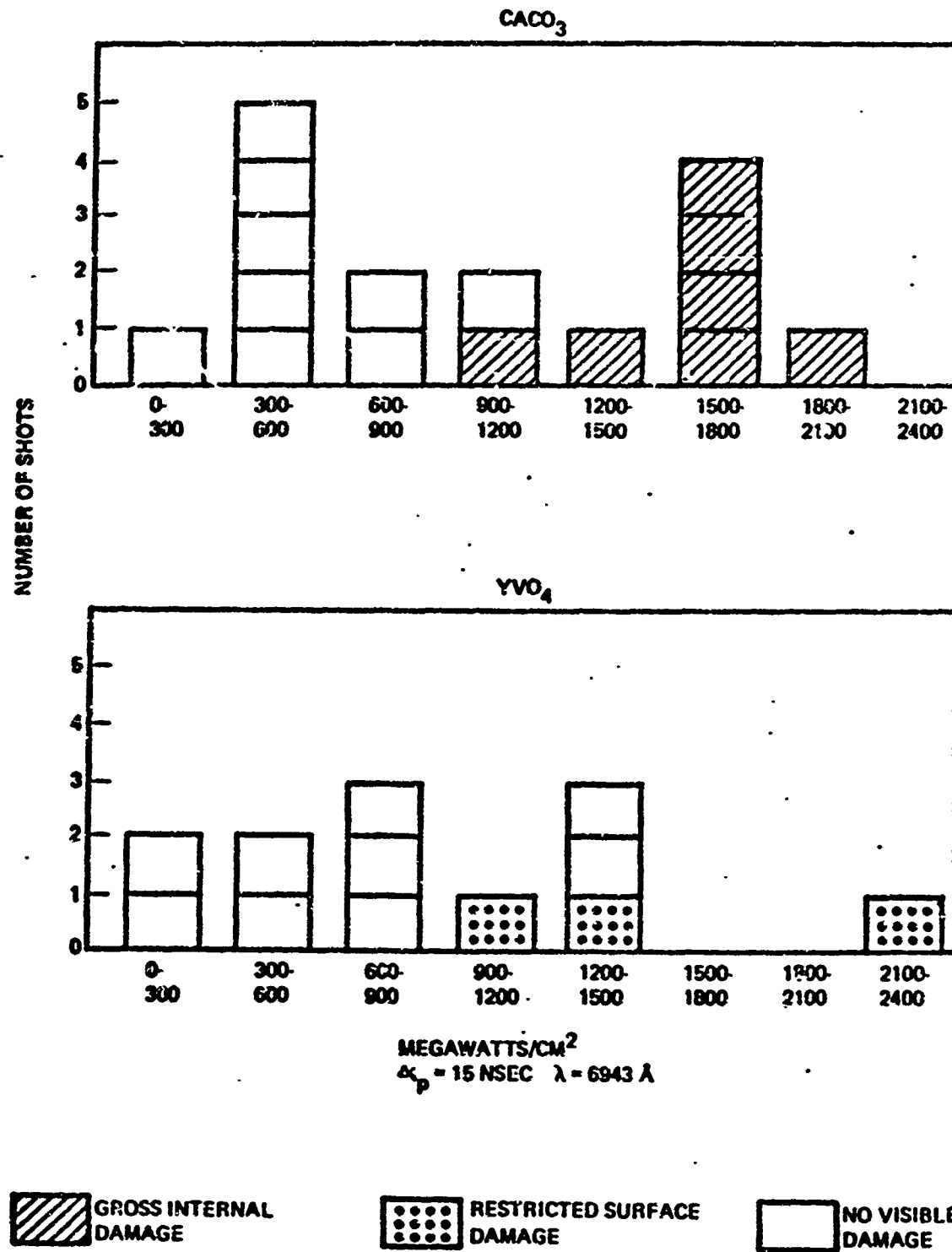


Figure 5-3. Comparison of Laser Damage Resistance for Calcite and  $\text{YVO}_4$

## REFERENCES

1. Kingery and Ludwig, J. Appl. Physics, 41, 370 (1970).
2. Milligan, Watt, and Rochford, J. Phys. Chem., 53, 227 (1949).
3. Milligan, W.O. and Vernon, L. W., J. Phys. Chem., 56, 145-8 (1952).
4. Broch, Zeit, Phys. Chem., 20B, 345 (1932).
5. Levine and Palilla, Appl. Phys. Letters, 5, 118 (1964).
6. Brecher, Phys. Rev., 155, 178 (1967).
7. Ballman, et al., U.S. Patent Re 26, 184 (1967).
8. Rubin and Van Uitert, J. Appl. Phys., 37, 2920 (1966).
9. Dess and Bolin, Paper presented at Electronics Materials Conference, Boston, Massachusetts (August 1966).
10. Witter, D. and Smith, M., Union Carbide Corporation, Private Communication (1970).
11. Stringer, J., J. Less-Common Metals, 8, 1-14 (1965).
12. Rostoker, W., The Metallurgy of Vanadium, Wiley, New York, 1958, p. 60.
13. Archard and Taylor, J. Sci., Inst., 25, 407 (1948).
14. "Optical Materials for Infrared Instrumentation", Report #2389-11-5, University of Michigan, January 1959.
15. "Glass Engineering Handbook," E. B. Shand, p. 40, McGraw-Hill Book Company, Inc., 1958.